Journal of Rock Mechanics and Geotechnical Engineering 6 (2014) 546–564

Contents lists available at ScienceDirect

Journal of Rock Mechanics and Geotechnical Engineering

journal homepage: www.rockgeotech.org

Full length article

Numerical analyses in the design of umbrella arch systems

J. Oke*, N. Vlachopoulos, M.S. Diederichs

GeoEngineering Centre, Queen's-RMC, K7L 3N6 Kingston, Canada

ARTICLE INFO

Article history:
Received 1 July 2014
Received in revised form
24 September 2014
Accepted 26 September 2014
Available online 21 November 2014

Keywords:
Forepole
Umbrella arch
Numerical modelling
Tunnel design
Numerical analysis

ABSTRACT

Due to advances in numerical modelling, it is possible to capture complex support-ground interaction in two dimensions and three dimensions for mechanical analysis of complex tunnel support systems, although such analysis may still be too complex for routine design calculations. One such system is the forepole element, installed within the umbrella arch temporary support system for tunnels, which warrants such support measures. A review of engineering literature illustrates that a lack of design standards exists regarding the use of forepole elements. Therefore, when designing such support, designers must employ complex numerical models combined with engineering judgement. With reference to past developments by others and new investigations conducted by the authors on the Driskos tunnel in Greece and the Istanbul metro, this paper illustrates how advanced numerical modelling tools can facilitate understanding of the influences of design parameters associated with the use of forepole elements. In addition, this paper highlights the complexity of the ground-support interaction when simulated with two-dimensional (2D) finite element software using a homogenous reinforced region, and three-dimensional (3D) finite difference software using structural elements. This paper further illustrates sequential optimisation of two design parameters (spacing and overlap) using numerical modelling. With regard to capturing system behaviour in the region between forepoles for the purpose of dimensioning spacing, this paper employs three distinctive advanced numerical models: particle codes, continuous finite element models with joint set and Voronoi blocks. Finally, to capture the behaviour/failure ahead of the tunnel face (overlap parameter), 2D axisymmetric models are employed. Finally, conclusions of 2D and 3D numerical assessment on the Driskos tunnel are drawn. The data enriched case study is examined to determine an optimum design, based on the proposed optimisation of design parameters, of forepole elements related to the site-specific considerations.

1. Introduction

As a design of underground excavations becomes larger and more complex, numerical analysis is required to combat increasingly difficult ground conditions, under which reinforcement may be required prior to excavation (pre-support). Due to its time and cost effectiveness in comparison with other pre-support methods (ground freezing, jet grouted columns, or pipe jacking), the umbrella arch method is increasing in popularity (Volkmann and Schubert, 2007). A corresponding increase in understanding of the interactions between the support system and the surrounding ground is required (Volkmann, 2003). Since 1991, literature has agreed that currently limited level of understanding is due to the lack of objective design criterion for the umbrella arch (Carrieri et al., 1991; Hoek, 1999; Volkmann, 2003; Kim et al., 2005; Volkmann et al., 2006; Volkmann and Schubert, 2006a, b, 2007, 2010; FHA, 2009; Hun, 2011; Peila, 2013). To aid design, Oke et al. (2014a) arranged the umbrella arch methods into thirteen sub-categories and associated them to applicable, specific failure mechanisms within the umbrella arch selection chart (UASC). This paper focuses on two of the sub-categories which employ the forepole element (confined and grouted in place) of the umbrella arch. It also illustrates the use of numerical modelling with regard to the overall response of the umbrella arch with forepole elements and the optimisation of selected design parameters for a squeezing failure mechanism, as illustrated in Fig. 1. Explicit numerical modelling for the optimisation of forepole element employed in other failure mechanisms, such as anisotropic conditions, is outside the scope of this paper. Investigation in the overall response of the forepole element was conducted using calibrated numerical models of two different tunnelling projects with in-situ data: the Driskos tunnel project (Vlachopoulos, 2009), and the Istanbul metro (Yasitli, 2013). Optimisation of selected design parameters was carried out for the severe squeezing ground at the Driskos tunnel at section 8 + 746 (Vlachopoulos and Diederichs, 2014).

* Corresponding author. Tel.: +1 6132178498.
E-mail address: jeffreyoke@gmail.com (J. Oke).

Peer review under responsibility of Institute of Rock and Soil Mechanics, Chinese Academy of Sciences.
1674-7755
http://dx.doi.org/10.1016/j.jrmge.2014.09.005

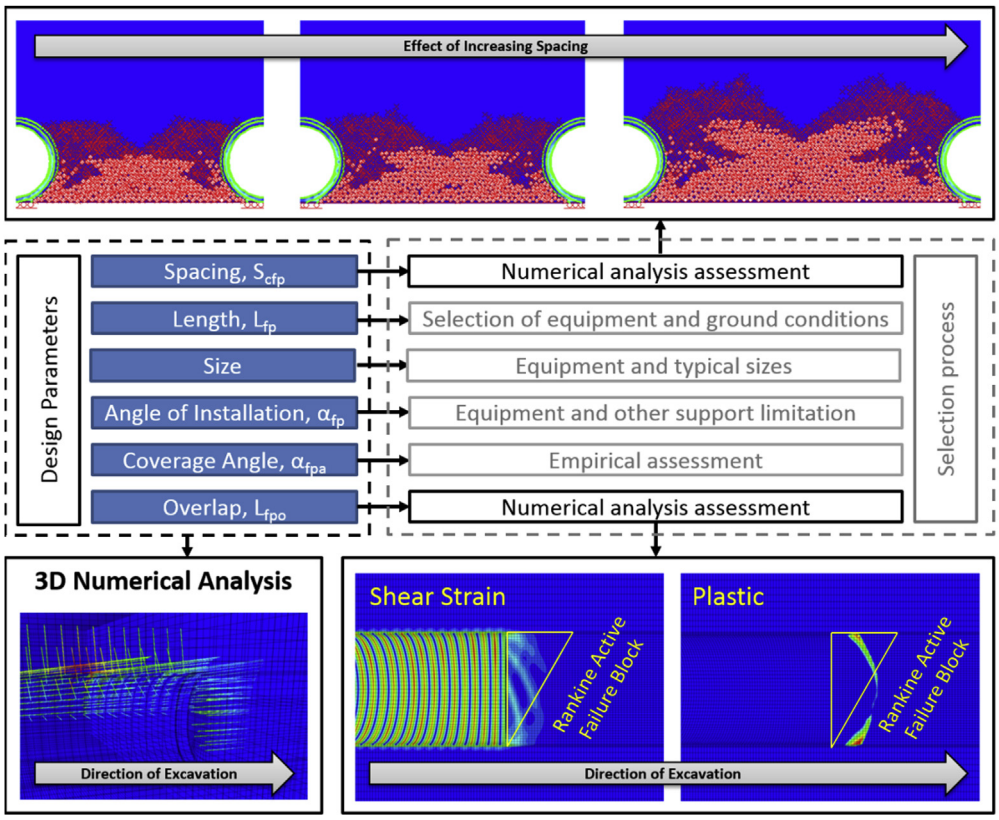

Fig. 1. Applications of numerical analysis for design parameters illustrated in Fig. 2, and overall response of forepole umbrella arch methods.

2. Background

Oke et al. (2014a) defined the umbrella arch as a pre-support installed within the tunnel, prior to the first pass of excavation, above and around the crown of the tunnel face which can be made up of spiles (length smaller than the height of excavation), forepoles (length greater than the height of excavation), or grout elements. This paper focuses specifically on the forepole elements, which are part of the temporary support system (e.g. shotcrete, steel sets, rockbolts, as shown in Fig. 2). However, prior to illustrating the extensive three-dimensional (3D) numerical analysis of forepole design, further details are necessary for the design parameters associated with the forepole umbrella arch, relevant investigations of cited literature that highlights important design considerations, the use of two-dimensional (2D) numerical investigation, and their disadvantages.

3. Design parameters

The design parameters for the forepole umbrella arch are shown in red in Fig. 2. Fig. 2a displays the length of forepole element (L_{fp}), and the length of forepole (or umbrella arch) overlap (L_{fpo}). The parameter L_{fp} cannot be optimised through numerical analysis as too many non-geomechanical factors governing the design exist. The L_{fp} depends on economic considerations, accuracy of drilling, accessibility of equipment and drillability with respect to ground conditions. The L_{fpo} can be optimised by using relevant numerical modelling. This overlap is required to ensure stability of the system and ground response, as illustrated in Fig. 1. In order to be effective in the longitudinal direction, the embedding of the forepole element requires sufficient distance (length) from the disturbed ground region. This embedment ensures that there will be sufficient longitudinal arching, which is the transfer of stresses at the tunnel face to the support system (in front of the face) and to the stable ground (ahead of the face), as illustrated in Fig. 3b. These parameters will be explained further in subsequent sections.

Fig. 2b illustrates the centre to centre spacing of the forepole elements (S_{cfp}), thickness of the forepole element (t_{fp}), and the outside diameter of the forepole element (ϕ_{fp}). The maximum S_{cfp} is defined by the requirement of developing a local arching effect, as shown in Fig. 3a (Volkmann and Schubert, 2007). This local arching can be analysed and captured with numerical models, as illustrated in the top portion of Fig. 1. It is important to note that the FHA (2009) has commented on the occurrence of a common misjudgement of the longitudinal (overestimation) and radial effects (underestimation) of the forepole design. Thus, there is a requirement for analyses on both a local (arching between forepole elements) and a global (complete system response) scale. The size of the forepole element is defined by two parameters: t_{fp} and ϕ_{fp}. Ultimately, these parameters will define the stiffness of the forepole as well as the loading area. This paper will illustrate that numerical modelling can be effective in determining an optimum size of the forepole elements within an umbrella arch arrangement. This optimum size, however, is further influenced by the installation equipment and the commercially standardised elements (pipes) available.

Fig. 2c displays the installation angle (α_{fp}) of the forepole element and the length of the unsupported span (L_{us}). The α_{fp} for spile element within umbrella arch methods can range from 5° to 40° as it is designed to lock in structural components or to ensure a certain thickness of grout barrier around the excavation. For forepole elements, however, the α_{fp} is defined by other temporary support elements (thicknesses of shotcrete and steel sets) as well as equipment clearances, to allow for the minimum possible angle.

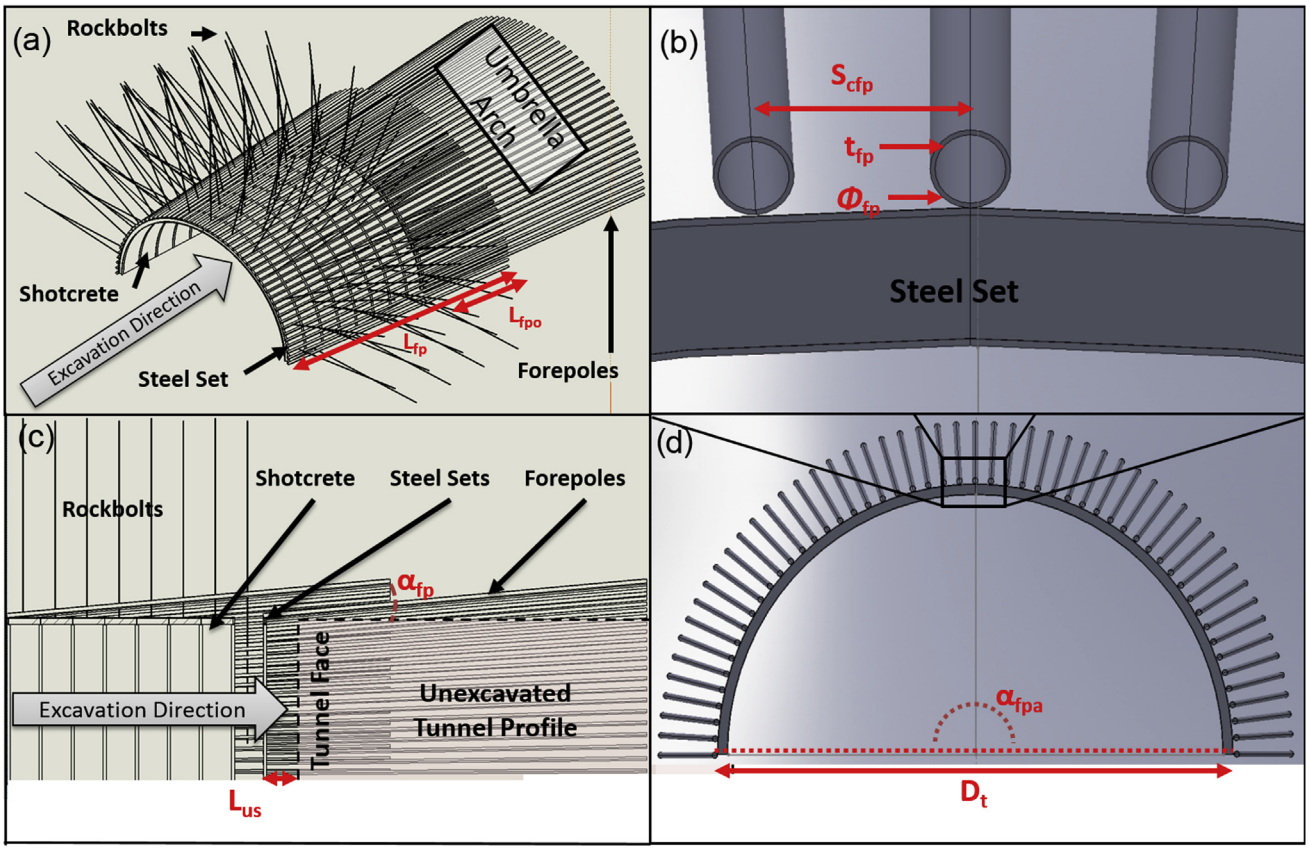

Fig. 2. Structural layout of the umbrella arch temporary support system with forepole elements. Red arrows and text indicate key design dimensions. (a) View of oblique support layout. L_{fp} is the length of forepole, and L_{fpo} is the length of forepole (or umbrella arch) overlap. (b) Viewport of (d). S_{cfp} is the centre to centre spacing of the forepole elements, t_{fp} is the thickness of the forepole element, and ϕ_{fp} is the outside diameter of the forepole element. (c) Profile view of support layout. α_{fp} is the installation angle of the forepole element, and L_{us} is the length of the unsupported span. (d) Cross-sectional view. D_t is the diameter of the tunnel, and α_{fpa} is the coverage angle of the forepole elements.

One must remember that the forepole elements and the umbrella arch support system are not employed in isolation and are used in conjunction with other support elements. The minimum possible angle of installation is deemed to be ideal as most cases result in failure of the ground material up to the forepole elements. When such failure occurs, a niche (or saw-tooth) profile is created, as shown in Fig. 4. This niche profile results in an increasing excavation size which consequently increases the requirement for more and/or larger other temporary support elements, neither of which is economical. The parameter L_{us} is typically defined by the steel sets spacing, although it is also important to take tunnel face stability into consideration when determining the L_{us}.

Fig. 2d defines the coverage angle of the forepole elements (α_{fpa}). The tunnel diameter, D_t, is a design parameter that defines the difference between a forepole element and a spile element, as previously mentioned. The α_{fpa} is defined by the failure mechanism more than the mechanical response of the system. For gravity driven failures, the forepole element only requires a α_{fpa} around the crown ($\sim$120°) of the excavation face to protect the workers working underneath. For subsidence driven failure mechanisms, it is more common to employ 180° coverage above the face of the tunnel (as shown in Fig. 2d). Similarly, Song et al. (2013) stated that 120° is optimal for weathered rock and 180° for soil. For squeezing ground conditions, Hoek (2001) suggested an increase of the

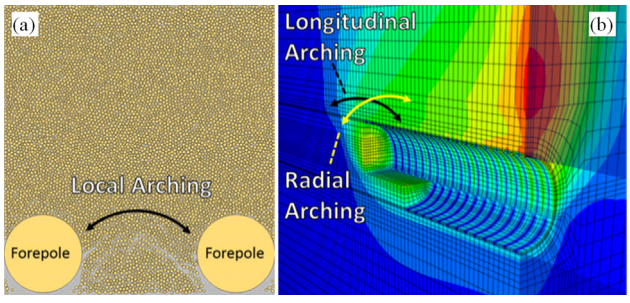

Fig. 3. Illustration of arching. (a) Local arching (modified after Doi et al. (2009)). (b) Longitudinal arching and radial arching.

Fig. 4. Niche (saw-tooth) profile construction due to the installation of umbrella arch with forepole elements.

coverage angle from 120° to 180° for severe to very severe squeezing conditions, respectively.

4. Literature investigations

While much of the previously discussed literature related to parameters is based primarily on empirical data, the following review sections summarise past work based primarily on numerical modelling. Design parameters based on modelling are summarised in Table 1.

4.1. Volkmann and Schubert (2006a)

Volkmann and his associated collaborators have carried out laboratory, in-situ, and numerical tests on the forepole element providing either commentary or analysis related to: cost comparison, sizes, length of forepole (L_{fp}), impact of in-situ measurement, disturbed ground foundation, length of forepole (or umbrella arch) overlap (L_{fpo}), and forepole installation methods. Due to the numerical focus of this paper, only the results of quantity, cost and sizes of the forepole elements will be further illustrated.

Volkmann and Schubert (2006a) described the passive response of the support, which requires displacement to mobilise the support effects. The stiffness (t_{fp} and φ_{fp}) of the support element requires less displacement to mobilise the support effects. The analysis of Volkmann and Schubert (2006a), however, did not take into consideration the local arching failure that could occur due to the increase of the spacing of forepole elements. The results of Volkmann and Schubert (2006a) and the arching statements from FHA (2009) reinforce the importance of a design process that incorporates the local and global responses of the system.

4.2. Song et al. (2013)

Song et al. (2013) carried out numerical and analytical analyses of a large-diameter steel-pipe-reinforced umbrella arching model with the parameters listed in Table 1. All of the analyses were compared to the factors of safety for bending (FOS_b) and shear (FOS_s). It must be noted that the other supports simulated in this numerical model were not changed (i.e. the shotcrete thickness was constant), and the effect of failing to consider this will be explained in subsequent sections.

The parametric analysis by Song et al. (2013) drew the following conclusions: (i) as ϕ_{fp} increased, FOS_s and FOS_b also increased; (ii) as the overburden depth increased, FOS_s and FOS_b decreased and converged; (iii) as S_{cfp} increased from 40 cm to 60 cm, FOS_s and FOS_b decreased; (iv) as the Young's modulus of the ground decreased, FOS_s and FOS_b also decreased. On the whole, the FOS_b was found to be more critical than FOS_s. The observations made by Song et al. (2013) suggest that FOS_b should be used as the primary indicator when evaluating the stability of the forepole elements.

4.3. Kim et al. (2005)

Kim et al. (2005) numerically analysed the effect of an umbrella arch when employing forepole elements within a grout zone around the outside of the excavation, with parameters outlined in Table 1. The forepoles used in this study were 60.8 mm in diameter, 3 mm in thickness, and 12 m in length. They were installed with a S_{cfp} of 0.4 m and L_{fpo} of 6 m, and the α_{fpa} of the umbrella arch was 120°. The grout was simulated by multiplying the original ground deformation modulus by a factor of 2. Their results showed a greater impact on reducing the surface settlement when employing the umbrella arch system in weaker ground condition (see Fig. 5), compared to instances that did not include the system (but other support was installed). Through a retrogressive analysis, their results further indicated that a prediction of surface and tunnel crown settlement is possible. However, their results did not agree with the surface settlement reduction plot found in the empirically driven UASC (Oke et al., 2014a) as shown in Fig. 5. A comparison of the results from Kim et al. (2005) with the surface reduction plot of Oke et al. (2014a) illustrates two important factors. Firstly, a parametric analysis with numerical models must be calibrated to a case study to bring any validity to the work and, secondly, due to the complexity of the umbrella arch system, it proves to be very challenging to be modelled numerically.

5. Numerical investigation

The authors have conducted 2D and 3D parametric analyses in order to illustrate the challenges of modelling forepole elements numerically. In each respective case, analyses were conducted by industry standard programmes: 2D numerical analyses were carried out by employing Phase2 v7 (Rocscience, 2010) and v8 (Rocscience, 2013); and 3D analyses were carried out by employing FLAC3D v4 (Itasca, 2009). These analyses also took into account deep and shallow tunnel excavations. The deep excavation was based on the parameters used in Vlachopoulos (2009) and Vlachopoulos et al. (2013) investigations of the Driskos tunnel of the Egnatia Odos highway in Greece. The parameters selected are from Section 4.3 of the Driskos tunnel where forepoles were employed in squeezing ground conditions of fractured flysch material. Selected ground parameters can be found in Table 2. The parameters provided the authors the opportunity to create a numerical model with previously verified input parameters (matched to average in-situ tunnel convergence). In an effort to further increase computational time, however, the simulation was simplified to a single circular tunnel excavation (full face), unless noted otherwise. An additional deep numerical model was also created based on a hypothetical squeezing case (hydrostatic condition at depth). The relevant general ground parameters of the generic squeezing model can be found in Table 2.

The shallow excavation runs performed were based on the in-situ surface settlement results and support design of the Istanbul

Table 1
Literature review summary of numerical parametric investigations.

Literature numerical analysis investigations	Centre to centre spacing, S_{cfp}	Thickness, t_{fp}	Diameter, ϕ_{fp}	Angle of installation, α_{fpa} (°)	Lateral earth pressure coefficient, K_0	Overburden (m)	Ground material
Volkmann and Schubert (2006a)	30 pieces of 114.3 mm × 6.3 mm forepoles had similar effects of reducing face and maximum settlement when compared to 20 pieces of 139.7 mm × 8.0 mm forepoles			–	–	–	–
Song et al. (2013)	40–60 cm	–	60–114.3 mm	20–180	0.4–0.6	10–40	–
Kim et al. (2005)	–	–	–	–	–	(0.5–3.0)D_t	Weathered soil – weathered rock

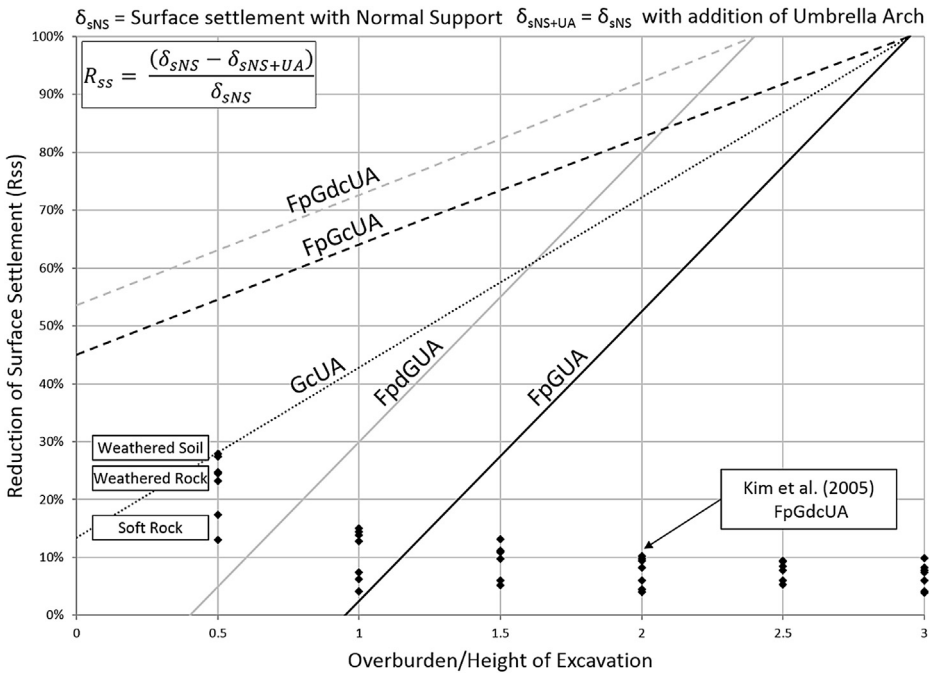

Fig. 5. Surface settlement reduction plot from the UASC (Oke et al., 2014a). Black diamonds indicate the results found from Kim et al. (2005). Note: FpGUA = forepole grouted umbrella arch; FpdGUA = double forepole grouted umbrella arch; FpGcUA = forepole continuous grouted umbrella arch; FpGdcUA = forepole double continuous grouted umbrella arch; GcUA = continuous grouted umbrella arch.

metro, as published in Yasitli (2013) and Ocak (2008). Two different sections of the Istanbul metro had similar geological profiles and structural layouts. The major difference, however, was that one section employed an umbrella arch system with forepoles while the other section did not. This difference allowed the authors to validate the support system for both scenarios, and instilled confidence that the parameters used to simulate the forepole element were realistic. The parameters used to simulate the ground condition for the Istanbul tunnel can be found in Table 2.

5.1. 2D numerical investigation

Literature concurred that 2D numerical analysis does not and cannot accurately simulate the response of forepole elements within an umbrella arch (Volkmann and Schubert, 2007; Peila, 2013). In order to illustrate this inability, two types of simulations were conducted to analyse the forepole elements within an umbrella arch. The first was a homogenous model, suggested by Hoek (2001) as a crude approach (Fig. 6a). The second was an "as-built" model where the forepoles were simulated explicitly (Fig. 6b). Fig. 6a illustrates that the stresses appear to capture the radial aching effect around the outside of the homogenous region, but the model is not able to capture the local arching between the structural elements. Furthermore, the homogenous model is not able to capture the longitudinal stress transfer. For the "as-built" model, no additional resistance to the deformation is provided by the forepole as shown in Fig. 6. Fig. 6d also illustrates the convergence of the unsupported, homogenous, multiple "as-built" simulated models and multiple 3D numerical model results. The homogenous model is the only one that is able to capture the expected reduction in the crown convergence when other support members are installed. Analysis of this model has found that while the homogenous model might capture empirical trends of reduction of the crown convergence, this method does not, however, capture the true longitudinal mechanical response of the umbrella arch. This is because when the forepole elements are installed without other supports, there is no significant reduction in the crown displacement, as denoted by the 3D analysis results (squares in Fig. 6d). Furthermore, Peila (2013) stated that it is difficult or impossible to define the improved ground conditions. The authors agree with Volkmann et al. (2006) that the only acceptable application of the homogenous model exists when grout is continuously connected around the outside of the excavation (with or without steel reinforcement). Despite of considerations of this type of umbrella arch, it remains difficult or impossible to correctly select the accurate stress release action required (Peila, 2013) to capture the

Table 2
Parameters used for numerical analysis. Materials were perfectly plastic, with no dilation. H_e is the height of excavation.

Case	Shape	D_t (or H_e) (m)	In-situ stress (or overburden)	Excavated material	Hoek-Brown parameters			Mohr-Coulomb parameters		Modulus of elasticity, E_{rm} (MPa)	Poisson's ratio
					m	s	a	c (kPa)	φ (°)		
Driskos tunnel (Vlachopoulos, 2009)	Circle	10	100 m	Flysch ($GSI = 31$)	0.66	0.000468	0.52	290	36	1442.1	0.25
Istanbul metro (Yasitli, 2013)	Horseshoe	6.8	10.75 m	Clay	–	–	–	20	33	38	0.33
Generic squeezing (Oke et al., 2014b)	Circle	10	3 MPa	Mudstone ($GSI = 20$)	0.345	0.0001	0.544	235	30.2	400	0.25

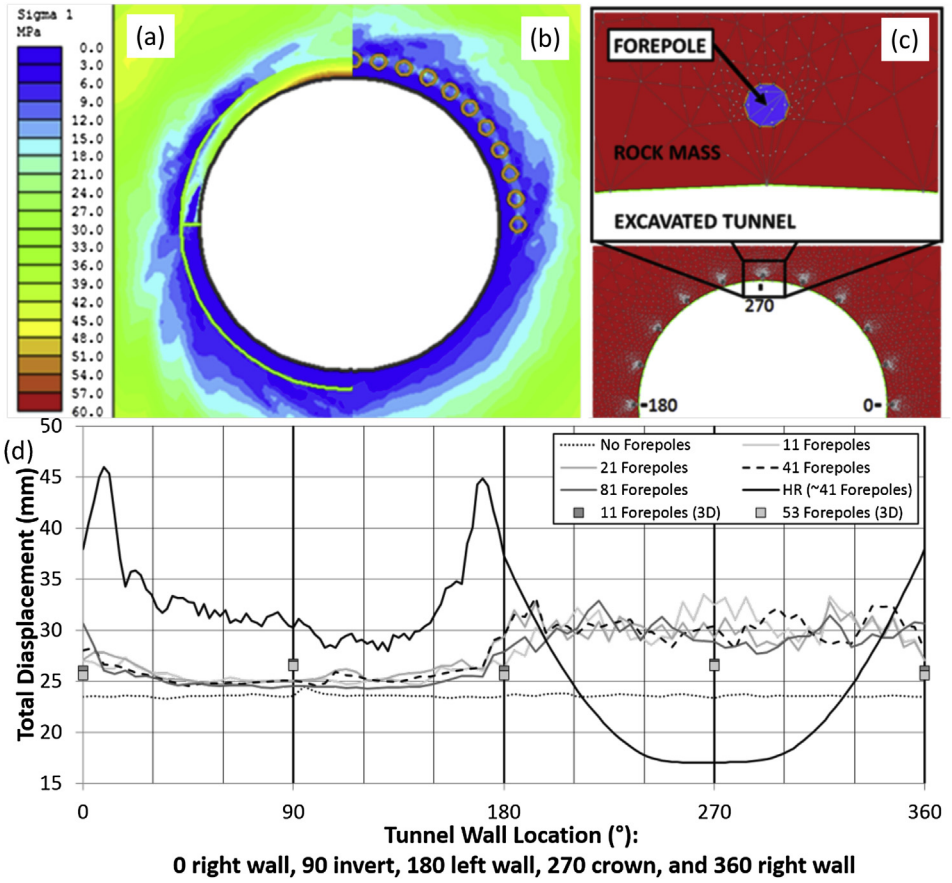

Fig. 6. Phase2 analysis of principal stress relocation due to forepoles models as: (a) homogenous model, and (b) "as-built" model. (c) Illustration of layout of 11 forepoles around top half of excavation (2D analysis). (d) Results of parametric 2D and 3D analyses of quantity of forepoles versus tunnel convergence.

3D tunnelling effect of the tunnel face, as explained in detail by Vlachopoulos and Diederichs (2014).

5.2. 3D numerical investigation

As previously explained, the authors conducted parametric analyses based on two different case studies to aid in the design and understanding of the forepole structural element. Both case studies have been simplified to single excavations with a constant excavation profile (no niche profile). The authors understood that such a simplification would, in turn, change the response of the Driskos tunnel excavation; however, the material and structural properties were selected from a previously calibrated numerical model. The changes of excavation process and tunnel profile would have a minimal impact on the already calibrated input parameters. Further simplifications to the numerical models will be stated in the following sections. Still, the authors conducted a parametric analysis on the interaction parameters for the forepole structural elements in order to fully understand their influence before any parametric analysis took place. The numerical mesh and boundary conditions for this analysis of the Driskos tunnel can be found in Fig. 7a–c.

The model set-up for the Driskos tunnel has a boundary width of $9D_t$ from the centre of the tunnel axis, and a longitudinal minimum boundary width of $4.5D_t$ (Fig. 7b). The boundaries are fixed at the bottom and at the entrance plane of the excavation in the normal direction. The top middle strip of the model is also fixed in the direction parallel to the tunnel axis (Fig. 7a and c). Stresses are applied on other boundaries to simulate gravity loads (Fig. 7a and c). The mesh was generated with a finer mesh (0.25 m) at the centre expanding to the peripheries. This primary numerical investigation of the Driskos tunnel simulated the forepole elements solely (no other support was simulated) in order to capture the independent influence of the support element, unless noted otherwise.

The numerical mesh of the Istanbul metro (Yasitli, 2013) can be found in Fig. 7d. It had similar model sizes and boundary conditions as the Driskos case except that a pressure of 100 kPa was applied to the surface (top) boundary to simulate the influence of building and traffic (Yasitli, 2013). The calibration of the Istanbul metro case was based on in-situ surface settlement results, which was also simplified to a single bore excavation. The simplification of the single bore excavation would cause an error within the numerical model, as the second excavation would influence the first one. To better understand this simplification, a simple 2D analysis was conducted. The authors utilised Phase2 v8 (Rocscience, 2013) to verify the impact of the twin tunnel excavation. A percent difference of 10% was found between the single excavation and double excavation when the umbrella arch method was not employed, as illustrated in Oke et al. (2013a). The calibration of the Istanbul tunnel and further parametric analysis will be explained in greater detail in the following section

5.2.1. Numerical investigation of forepole element

FLAC3D v4 (Itasca, 2009) possesses three different types of structural elements which can all be employed to simulate the individual forepole elements. These existing structural elements are CableSel, BeamSel, and PileSel (Fig. 8a). The CableSel element is capable of bearing axial loading only, and is not able to capture the

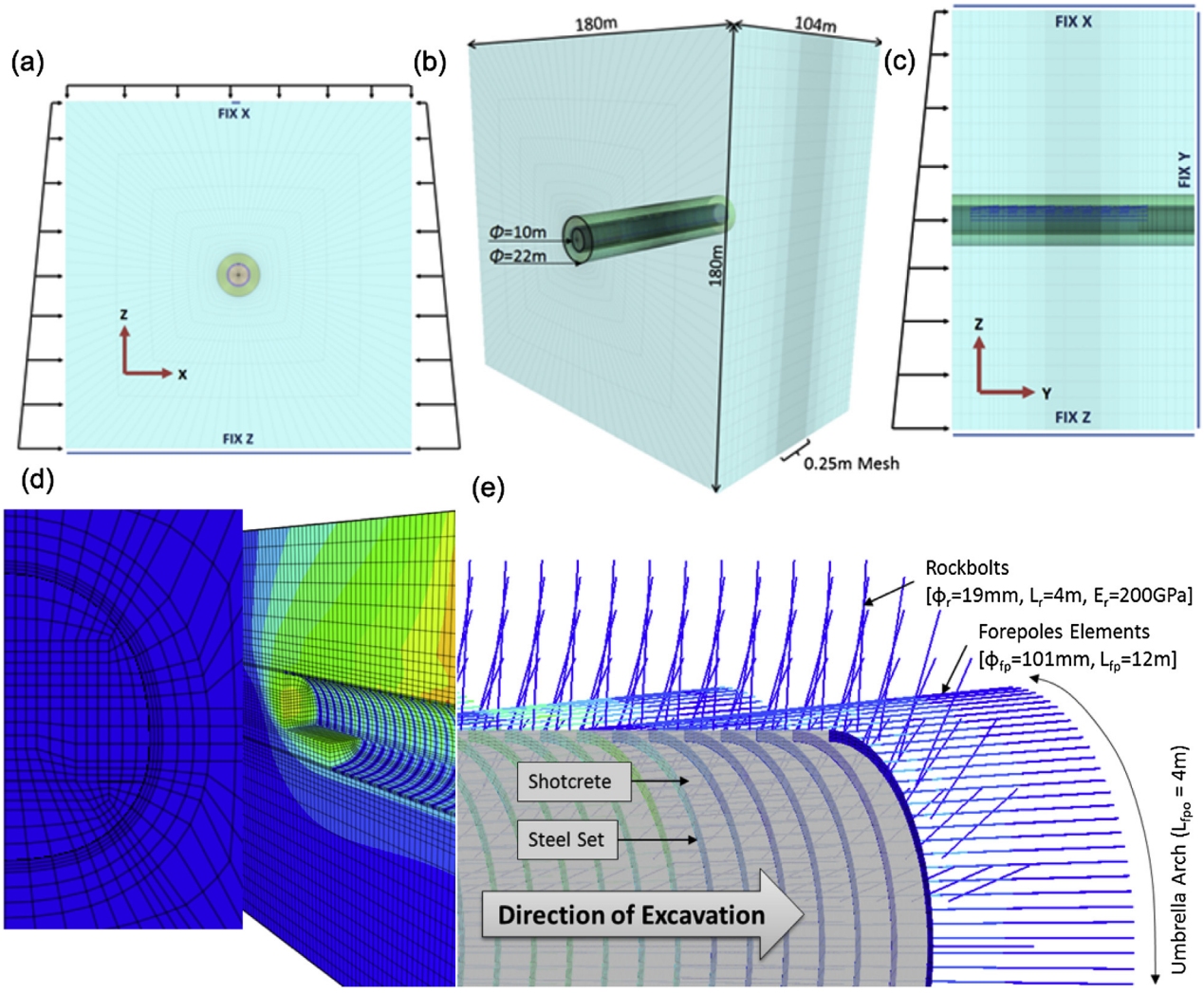

Fig. 7. 3D numerical models used within this paper. (a)–(c) Driskos tunnel; (d) Istanbul metro; and (e) Generic numerical model.

longitudinal bending/stress transfer response of a forepole element. The BeamSel element is capable of taking on both axial and bending forces; essentially, the PileSel is a BeamSel element with the additional "rock-bolt logic". The "rock-bolt logic" allows for the ability of the support element to account for changes in confining stress around the reinforcement, strain-softening behaviour of the material between the pile and the grid, and tensile rupture of the pile (Itasca, 2009). The slider constitutive model follows a Mohr-Coulomb failure criterion and the spring is defined by its stiffness parameter (Fig. 8c). The authors have found that the PileSel is the most suitable for the simulation of the forepole element, in agreement with other authors (Broch et al., 2006; Volkmann and Schubert, 2006a; Vlachopoulos and Diederichs, 2014) who have studied numerically the umbrella arch systems.

The concern that the PileSel element presents lies in the requirement that exact values of the interaction parameters must be selected (especially that of the stiffness parameter, Fig. 8c). Itasca (2009) suggested that these interaction parameters should be obtained from laboratory tests, yet, if laboratory testing of this nature is not possible, as is the case in most investigations, the stiffness parameter can be approximated by the method introduced by St. John and Van Dillen (1983). A simplified version of the St. John and Van Dillen (1983) equation (Eq. (1)) has been established to provide a reasonable calculation for the stiffness parameter, according to Itasca (2009). In addition, this simplification has a one-tenth factor which helps to account for the relative displacement that occurs between the structural element and the borehole surface (the annulus), as illustrated in Fig. 8b. The material properties regarding grout are not always provided, as is the cases of the Istanbul metro from Yasitli (2013) and the Driskos tunnel from Vlachopoulos (2009). Therefore, Itasca (2009) suggested as a general rule that the stiffness parameter be set to ten times the equivalent stiffness of the stiffest neighbouring zone (Eq. (2), with m value of 1). The stiffest neighbouring zone will always be the forepole element.

$$k = \frac{2\pi G}{10 \ln\left(1 + \frac{2t_a}{\phi_{fp}}\right)} \tag{1}$$

$$k = 10^m E_f \tag{2}$$

where G is the shear modulus of surrounding material (usually grout), t_a is the thickness of the annulus, m is the stiffness multiplier, and E_f is the modulus of elasticity of the forepole element.

Identification of the correct stiffness parameter is essential. If the selected stiffness parameter is too low, the deformation of rock

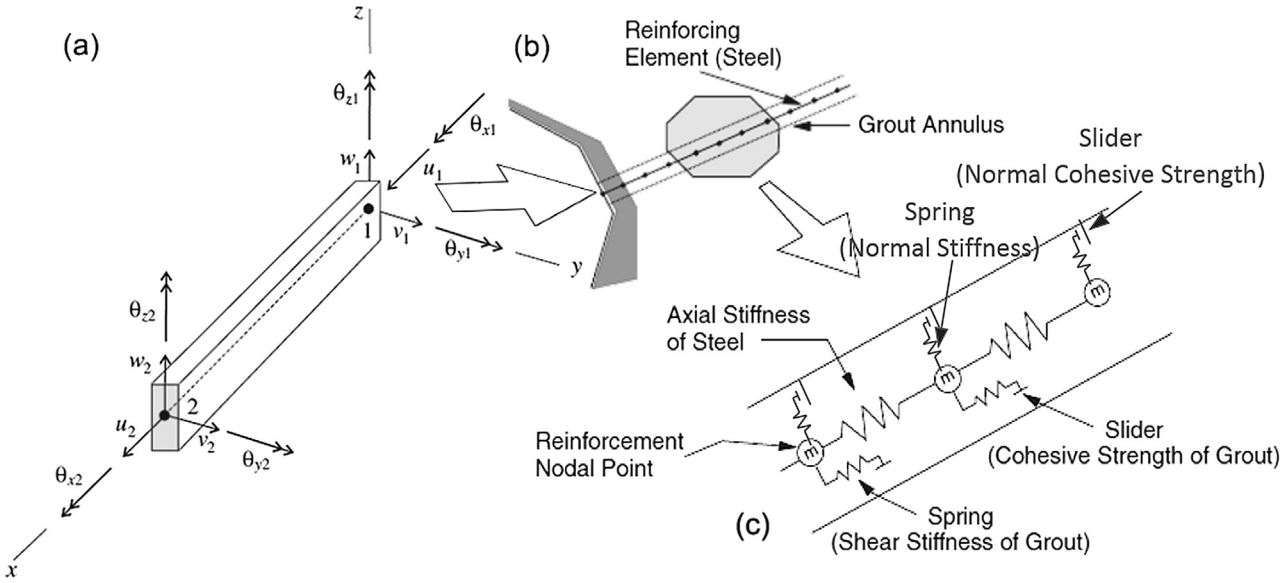

Fig. 8. Illustration of the PileSel element in FLAC3D: (a) beam-column element; (b) nodal division; and (c) interaction parameters. Illustration is modified after Itasca (2009).

mass is beyond that of the support element, without capturing the true interactions. Conversely, if the stiffness parameter is too great, numerical instability is possible. Numerical instability is the result of the failure criteria of the interaction connection (slider) constantly resulting in failure with any slight movement of the numerical mesh around the structural element. An example of this sensitivity can be found in Fig. 9. Fig. 9 shows the displacement profile of the complete forpole element with 2 m having been excavated at the front end of the support element. The ensuing results are from adjustments of the interaction parameter by a factor of 10 for the generic squeezing numerical model, as previously described. The results illustrate that the greatest magnitude of deflection in this simulation was found when $m = 0$ and the cohesion, c, a parameter in the normal interaction direction was set to zero. When the value of m increased or decreased from $m = 0$, the maximum deflection value decreased.

The interaction parameters for the forepole element of the Driskos tunnel were investigated in an effort to illustrate the sensitivity of each parameter, as shown in Table 3. The base model employed the parameters suggested by Itasca (2009) and the lowest values (expect practically zero values) were found in the literature (Trinh, 2006). The lower values of the sensitivity analysis were based on a zero or practically zero value and the higher values were based on the highest values found in the literature (Vlachopoulos (2009) for FLAC3D and Funatsu et al. (2008) for particle flow code (PFC) (Itasca, 2002)) or a multiplication of the base value. An illustration of the interaction parameters between the pile elements and the numerical mesh can be found in Fig. 8c.

The results of this sensitivity analysis are illustrated in Figs. 10 and 11. Fig. 10 displays the results of the sensitivity analysis of the tunnel convergence recorded at the tunnel face and at the distance three times of the tunnel diameter away from the tunnel face ($3D_t$). The parameters which show an influence on the tunnel convergence in Fig. 10 are plotted in Fig. 11. Fig. 11 presents the different displacement profiles captured in the sensitivity analysis. The most notable analyses from Fig. 11 are Run 12 and Run 8. Run 12 has a practically zero value for the normal stiffness value of k_n. Due to such a low k_n, little or no stress interaction occurs between the supports of the deforming ground. The results from Run 12 suggest that the majority of mechanical response from the forepole element comes from the normal stress interaction. Run 8 illustrates that the interaction parameter failure occurs between the forepole

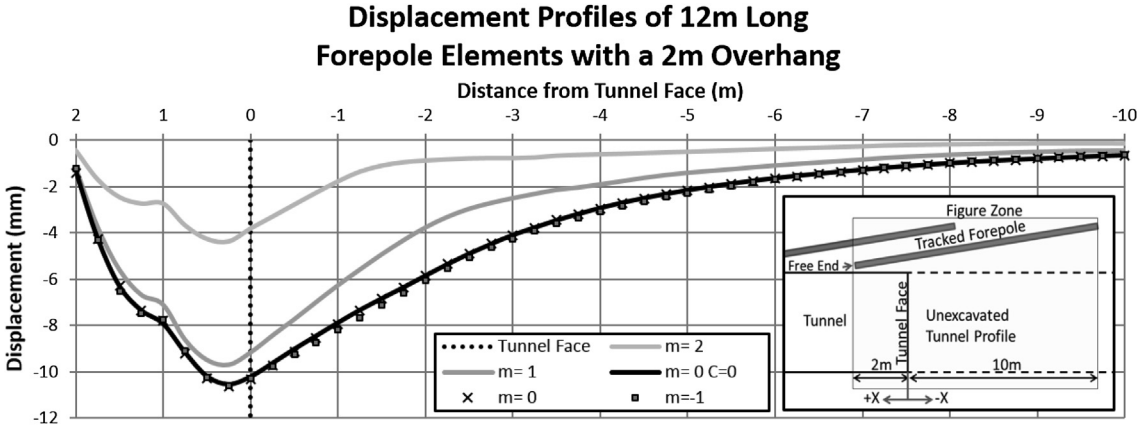

Fig. 9. Parametric analysis of interaction stiffness parameter in order to determine the maximum displacement for a forepole element for the generic squeezing numerical model. Positive distance is within the excavated zone and negative distance is in the unexcavated zone of the tunnel profile. c is the cohesion, $k = 10^m E_f$, where $E_f = 200$ GPa.

Table 3
Interaction parameters for the sensitivity analysis of the PileSel interaction parameters with the associated analysis runs.

Interaction parameters							
FLAC3D code	cs_scoh	cs_sfric	cs_sk	cs_ncoh	cs_nfric	cs_nk	cs_ngap
Symbol	c_s	φ_s	k_s	c_n	φ_n	k_n	g
Units	[F/L]	(degrees)	[F/L^2]	[F/L]	(degrees)	[F/L^2]	On/off
Base	[a]$c\phi_{fp}\pi$	[a]φ	[c]1.0×10^7	[a]$c\phi_{fp}\pi$	[a]φ	[c]1.0×10^9	Off
High value	$2c\phi_{fp}\pi$	2φ	[b]1.0×10^{11}	$2c\phi_{fp}\pi$	2φ	[d]1.0×10^{12}	On
Low value	0	0	0	[c]0	0	0	
High run#	Run 1	Run 3	Run 5	Run 7	Run 9	Run 11	Run 13
Low run#	Run 2	Run 4	Run 6	Run 8	Run 10	Run 12	

Note: c_s is the cohesion in shear direction, φ_s is the angle of friction in shear direction, k_s is the stiffness in shear direction, c_n is the cohesion in normal direction, φ_n is the angle of friction in normal direction, k_n is the stiffness in normal direction, "g" represents the gap, c is the cohesion of ground material, ϕ_{fp} is the outside diameter of the forepole element, and φ is the friction angle (Trinh, 2006; Funatsu et al., 2008; Itasca, 2009; Vlachopoulos, 2009).

and the tunnel face, allowing the ground material "flow" around the structural element. The results of this sensitivity analysis find that the parameter k_n will govern the deflection profile of the forepole element. Furthermore, the cohesion, c_s, and the shear stiffness, k_s, are the second and third most influential parameters, respectively.

The authors utilised the lessons gleaned from the interaction sensitivity analysis to calibrate the Istanbul metro case study. In order to calibrate the numerical model, the k value (normal and shear) was adjusted for all structural elements in situations involving tunnels built without forepole elements. This situation was captured within 5% of the in-situ data, which is in acceptable limits of possible error due to the aforementioned simplification of the single tunnel excavation. The calibration of the model with the forepole element required a more intensive process as illustrated in Fig. 12. Fig. 12 represents the three step process carried out in order to find the greatest impact on reducing surface settlement due to the installation of the forepole element. First, the k_s and k_n multiplier, m, was increased (denoted by the black squares in Fig. 12) from 1 until it became evident that the minimum surface settlement was present. This minimum value occurred when the stiffness multiplier was 4. Next, the normal multiplier was kept constant at $m = 4$ while the k_s parameter multiplier was varied from 1 to 6, as denoted by the black diamonds in Fig. 12. As is illustrated, there was no change in the ground surface settlement until the k_s parameter multiplier became greater than 4. In the third of three steps, the shear multiplier was held constant at $m = 4$ while the k_n parameter multiplier varied from 2 to 5, as denoted by the black triangles in Fig. 12. The smallest amount of surface settlement was captured when the k_n multiplier was reduced to 3. Consideration of these results dictated that the forepole elements' shear and normal

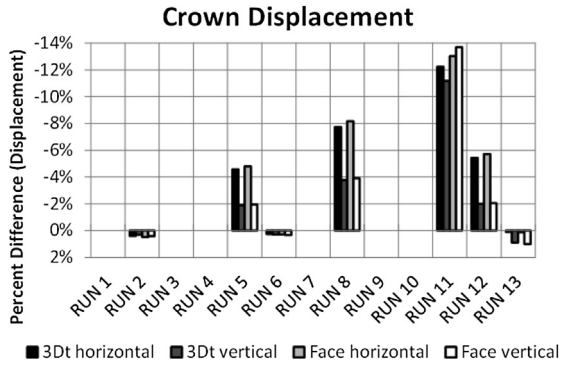

Fig. 10. Percent difference of displacement with baseline interaction parameters values. $3D_t$ denotes the measurement of the convergence conducted at the distance three times of the tunnel diameter away from the tunnel face. Interaction parameters for each run can be found in Table 3 (modified from Oke et al. (2012)).

stiffness multipliers were set to 4 and 3, respectively, for analysis of the design parameters of the Istanbul metro. The calibrated numerical model with forepole elements was within 25% of the in-situ results, a difference of only 10 mm. Such a minor difference can be credited to an inaccurate capture of the interaction between the forepole element and other structural support members, as explained in the subsequent section.

Broch et al. (2006) found that a fixed connection between the spile elements and other supports could reduce the displacement ahead of the tunnel face by 80%, when compared to the un-fixed (free) numerical analysis. However, it remains the authors' opinion that a forepole embedded into shotcrete forms an elastic or plastic connection, not a fixed connection. To date, FLAC3D does not support multiple-layered interaction connection (Itasca, 2009), which makes an elastic/plastic connection difficult to be incorporated. In lieu of this, the authors felt that a free connection would most closely represent reality.

5.2.2. Design parameters investigation

As previously discussed, a parametric investigation in the Driskos tunnel and the Istanbul metro was conducted to illustrate the influence of each design parameter: S_{cfp}, α_{fpa}, the size/stiffness of the forepole element, α_{fp}, L_{fpo}, and the effect of other supports and geometry.

(1) Centre to centre spacing, S_{cfp}

Centre to centre spacing, S_{cfp}, of the forepole element of an umbrella arch was investigated by increasing the number of forepole elements that spanned a coverage angle of 180° from 3 to 157. Fig. 13a illustrates the results of this analysis. An increase in the number of forepoles from 3 to 53 yields a displacement at the free end of the forepole of 18% difference (denoted by the diamond markers within the embedded chart of Fig. 13a). Despite of this, there remains only a 5% difference of displacement when the number of foreploes was increased from 53 to 157 (denoted by the square markers within the embedded chart of Fig. 13a). Therefore, the addition of more forepoles in an effort to control deformation beyond this threshold is, perhaps, not significantly advantageous when balancing material cost and operational cost (as noted previously in the investigation of spacing by Volkmann and Schubert (2006a)). It is important to note that the mesh size of the numerical model was 0.25 m at the tunnel boundary, which is nearly equal to S_{cfp} of the 63 forepoles. Thus, after the number of forepoles is greater than 53 (~0.3 m spacing), minimal impact is induced by the mesh size of the numerical mode. Furthermore, as the numerical model used was a continuous model, failure that would most likely occur between elements with larger spacing was not captured, rendering the results of this numerical analysis applicable

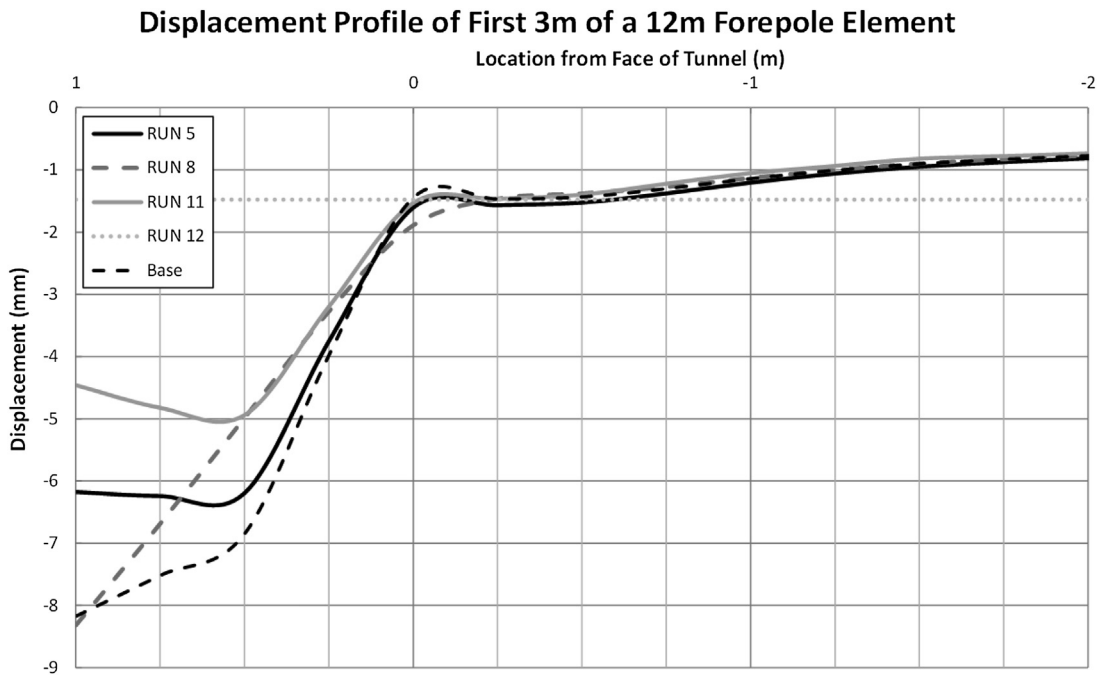

Fig. 11. Displacement profiles of the first 3 m of a 12 m forepole element obtained by numerical analysis with 1 m of overhang. Runs that are too similar to base results are not shown in the chart. Interaction parameters for each run number can be found in Table 3.

only for stable (at the tunnel face) squeezing ground conditions, such as the Driskos case.

S_{cfp} was further investigated by employing the numerical model based on the Istanbul metro ($\alpha_{fpa} \approx 170^{\circ}$, $S_{cfp} = 40$ cm, $\phi_{fp} = 114$ mm). A numerical analysis was carried out to investigate the effect of varying centre to centre spacing from 26 cm to 50 cm while simultaneously changing the coverage angle from 90° to 200°. Twenty four cases were analysed to allow for a higher resolution of natural neighbour interpolation of data points with the ranges examined. The results of these analyses (see Fig. 14) illustrate a slight difference in reduction of surface settlement with the effect of spacing in comparison to the coverage angle. It is found that the coverage angle has a greater influence than the spacing of the forepole element on the global response of the system. It is also apparent from raw data, however, that the 40 cm spacing is capable of controlling settlement more effectively than spacing with an equivalent coverage angle of up to 160°, indicating an optimum spacing value. Once again, however, this analysis was unsuccessful at capturing the local failure between the support elements (due to mesh size), and the interaction parameters were only calibrated to a spacing of 40 cm. According to these results, the stress redistribution caused by installation of the forepole elements were captured, as illustrated in Fig. 15. Fig. 15 displays the final displacement of three different points around the tunnel cavity for varying coverage angles while maintaining constant spacing (40 cm). The results find that the stresses are first redistributed at the side walls, causing great deformations. As the coverage angle increases, the stresses are transferred away from the excavation walls to below the excavation due to the support, decreasing the convergence of the side walls further, which explains why the coverage angle has a greater impact on the global response.

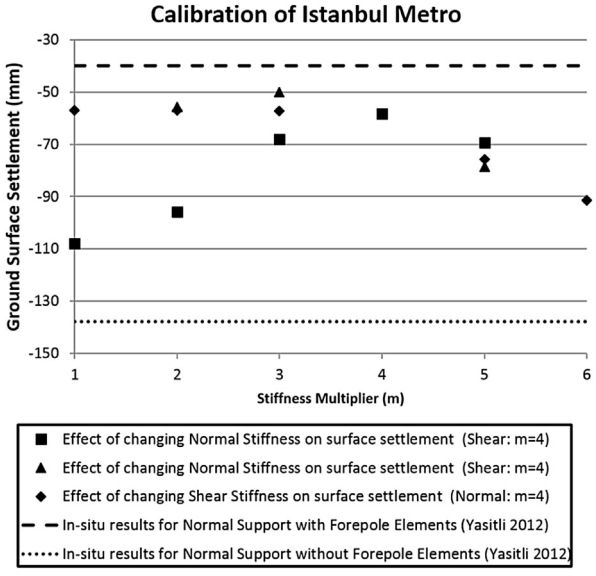

Fig. 12. Numerical results of the Istanbul metro for calibration of the normal and shear stiffness interaction parameters.

(2) Size/stiffness of the forepole element

A parametric analysis based on the Driskos tunnel was also conducted on the size of the forepole element. The value of ϕ_{fp} was selected to capture the full range of acceptable forepole sizes. The smallest diameter was that of the largest standard size rebar used in Europe (50 mm). The range of forepole metal pipes used in the analysis was the values cited in the literature. Intermediate sizes were also evaluated in order to determine the effects of a constant t_{fp} (6.5 mm) while simultaneously altering the value of ϕ_{fp}, and a constant ϕ_{fp} (141 mm) while altering the value of t_{fp}. These numerical changes in the size of the forepole element, however, only affect the stresses being applied to the structural element (surface area) and the stiffness of the structural element. The purpose of these numerical runs tried to determine the existence of an optimal range of forepole size. Forepole elements require a minimisation of stress concentrations to ensure a large enough exposed perimeter to

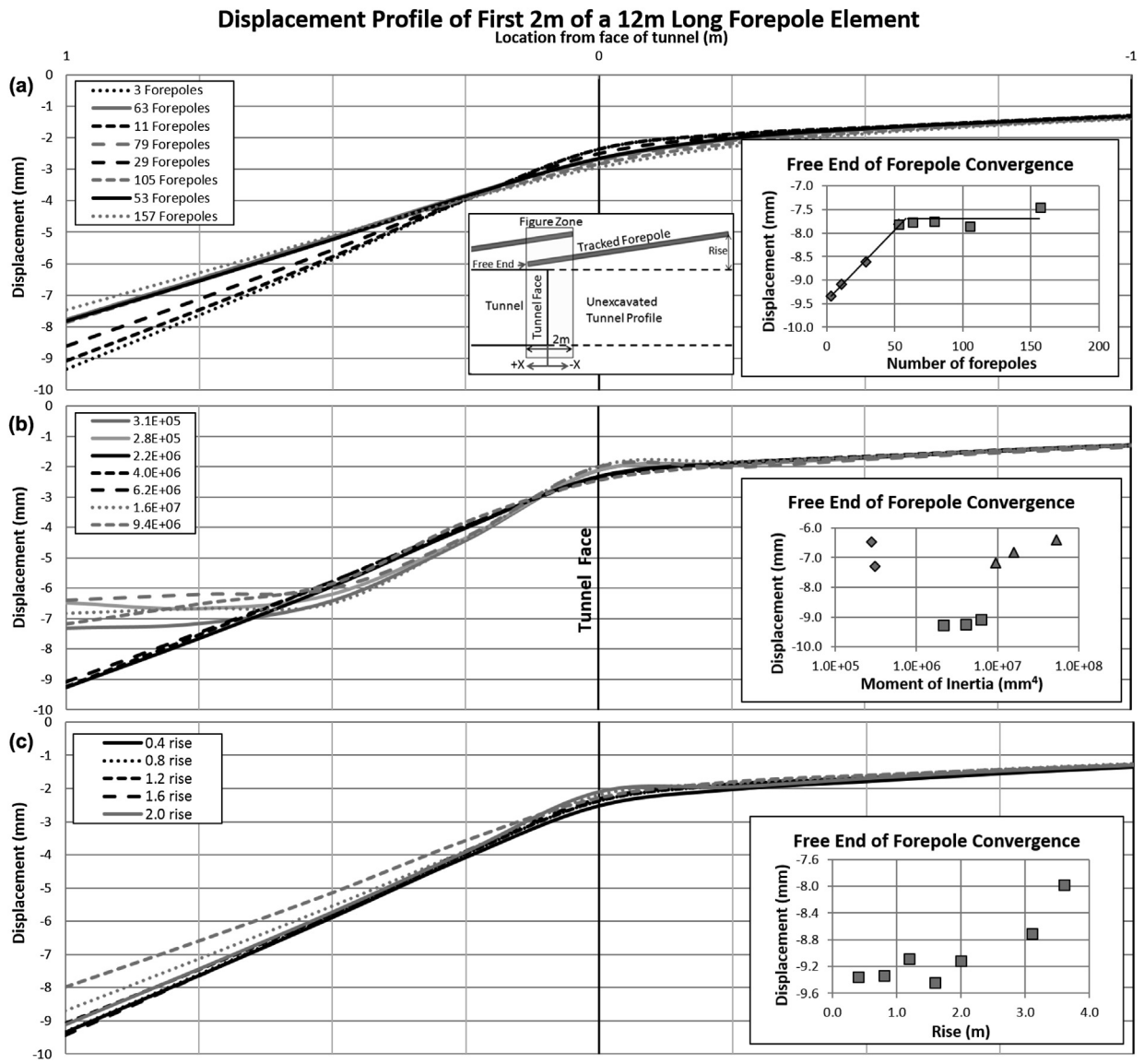

Fig. 13. Displacement profiles of the first 2 m of a forepole element based on 3D numerical analysis with the Driskos tunnel parameters. The plot illustrates the values of displacement of the free end of the forepole with varying number of forepoles: (a) effect of number of forepoles; (b) effect of forepole size; and (c) effect of angle of installation.

disperse stresses, but must be simultaneously small enough to move with the ground. The result of this analysis can be found in Fig. 13b. The optimum size for ϕ_{fp} was 101–141 mm, with a t_{fp} of 4–6.5 mm, which resulted in a moment of inertia range of $(2.2–6.2) \times 10^6$ mm^4 as denoted with black lines in Fig. 13b as well as the squares within the imbedded image.

(3) Angle of installation

The angle of installation (α_{fp}) was also investigated using the Driskos tunnel numerical model. The change of α_{fp} was adjusted by

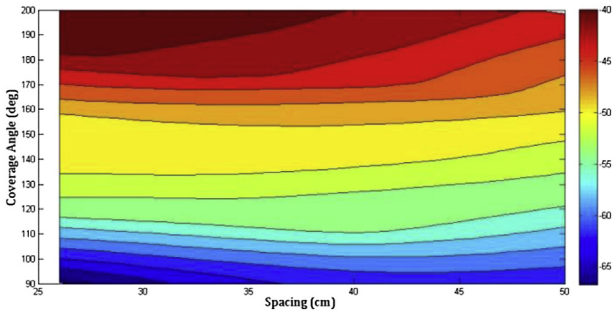

Fig. 14. The effects of centre to centre spacing and coverage angle on surface settlement based on numerical models (parametric analyses of 24 cases) of the Istanbul metro.

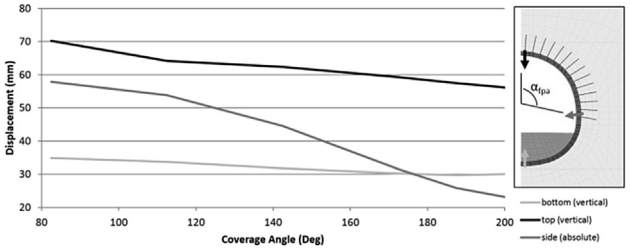

Fig. 15. Effect of coverage angle on displacement for a 40 cm forepole spacing for the Istanbul metro analysis. Right embedded image displays a α_{fpa} of 200°, and the arrows illustrate the location of referenced displacement to the respected colour.

increasing the rise (offset length normal to the tunnel boundary) of the forepole element. The lowest rise was set to capture the extreme case whereby the forepoles were separated by 12 cm (to allow for the application of shotcrete and other relevant supports, and accessibility of equipment). The rise was increased slightly in order to capture the typical installation angles (3°–7°). Further incremental runs were conducted until a rise of 3.6 m was achieved, in an effort to capture an installation angle greater than 15°. Such an analysis indicated that increasing the installation angle of forepole will decrease the displacement of the forepole. On average, the forepole also experienced 2.6 mm of displacement at the face. Conversely, a decrease in convergence was observed at the tunnel face (3.51%) and $3D_t$ from the face (2.82%) as the rise was increased from 0.4 m to 3.6 m. Within the forepole structural element itself, the numerical analysis captured a compression of 800 N for 0.4 m rise, which is in sharp contrast to a recorded tension of 4200 N for the 3.6 m rise. It can be postulated that with an increased angle, the forepole would act in a mode similar to that of a rockbolt rather than purely a forepole function. This conclusion is conducive with rockbolt design logic, usually most effective when the rockbolts are installed normal to the tunnel axis and take on tension, while forepoles bear axial compression force (Volkmann and Schubert, 2007).

The niche profile is defined by the angle α_{fp}, which creates a greater excavation opening with a larger angle. This analysis did not, however, simulate the niche profile and as such, did not capture the effect of the increasing excavation opening size with the increasing α_{fp}. From the authors' collective experiences, the minimal improvement to convergence for the numerical model does not outweigh the potential for further convergences based on the absent assumptions of the numerical model. Thus, the authors conclude from this analysis that the α_{fp} of a forepole element should not diverge significantly from the horizontal plane unless structural analysis is conducted to ensure that the support is analysed in accordance with various modes of failure. The results of this analysis can be found in Fig. 13c.

(4) Overlap of umbrella arch

An investigation was carried out to determine the effect of overlap of the umbrella arch, L_{fpo}, design for the Istanbul metro ($L_{fpo} = 3$ m, $L_{fp} = 12$ m). This analysis, however, was modified to a full face excavation in order to remove the influence of staged excavation (i.e. top heading and bench) on the tunnel face and to promote more convergence at the tunnel face. Different overlaps of 0 m, 3 m, 4 m, 5 m and 6 m were selected for the analysis. Fig. 16 illustrates the improving trend of L_{fpo} when (a) the density of the face reinforcement has been kept consistent with the original design and (b) the face reinforcement is not altered from the original design (support only installed within top heading region). In both cases, the surface settlement of the numerical model converges when L_{fpo} is greater than the Rankine block failure distance (RFD) (i.e. the distance away from the face that the RFD passes), as illustrated in Shin et al. (2008), Wang and Jia (2008), and Volkmann and Schubert (2010). This finding indicates that, in order to optimise the effect of umbrella arch on surface settlement, forepoles should always be installed just past the failure zone distance, ahead of the tunnel face. Furthermore, it was found when the umbrella arch was not installed, there was only a 13% improvement of the surface settlement by increasing the face reinforcement from case (b) to case (a). Comparably, when the umbrella arch was installed (3 m of overlap only), there was a 58% improvement of surface settlement when the face reinforcement was increased from case (b) to case (a), as shown in Fig. 16. Such differences regarding surface settlement between the two face reinforcement patterns are

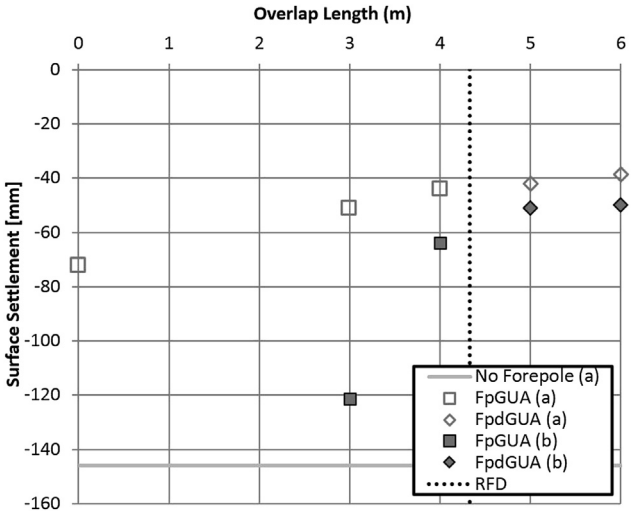

Fig. 16. Effect of overlap on the Istanbul metro with a full face excavation.

caused by the redistribution of stresses at the invert of the tunnel, resulting in larger displacements at the bottom of the tunnel face. These results indicate the importance of well-designed face reinforcements and the requirement for further investigation of the impact of face reinforcement and umbrella arch interaction.

The effect of the overlap was also investigated with the generic squeezing numerical model. Two cases were numerically analysed, the first with a 4 m overlap and the second without overlap. The deflection profiles of the two numerical models are plotted in Fig. 17 where only 1 m of the forepole element is shown. The location of the free end of the forepole element was 2 m from the tunnel face. The analytical models proposed by Oke et al. (2014b) were calibrated to the two different cases by the least square analysis for both loading conditions defined by the longitudinal displacement profile (LDP) by Vlachopoulos and Diederichs (2014) and the modified LDP by Oke et al. (2013b). It was therefore determined that by curve fitting of the deflection profile, a factor (0.5 and 0.4 for the LDP and the modified LDP, respectively) of the loading condition within the region of the overlap was required in

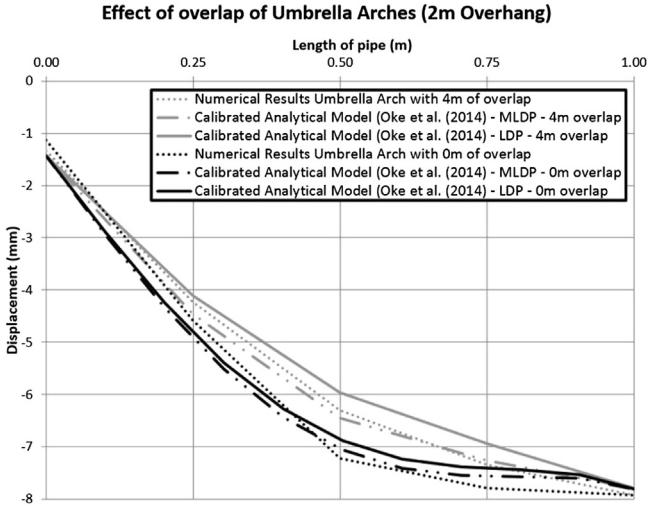

Fig. 17. Results of numerical models based on the generic squeezing tunnel and semi-analytical models based on the proposed model of Oke et al. (2014b). The 4 m overlap case had a loading condition reduced by a factor of 0.5 and 0.4 for the LDP and modified LDP, respectively.

order to match profiles. This is a promising result which captures the additional benefits of the overlap. However, additional investigation is required with regard to in-situ results in order to further quantify and validate this reduction of the loading condition. The analytical process is outside the scope of this paper, and will not be further discussed within this paper. Further explanation of this analytical process can be found in Oke et al. (2014b).

(5) Other support elements and geometry

The impact of additional temporary support elements on the response of the umbrella arch support system has been found to be critical. The empirical evidence used to create the UASC (Oke et al., 2014a) shows that with increasing overburden, there should be a greater reduction in surface settlement. However, the numerical model of the Istanbul metro illustrates that changing the overburden by 2 m induced an increase of 19% of surface settlement, as denoted by the 5 solid black outlined squares in Fig. 18 (Oke et al., 2014c). This increase can be attributed to the 30% increase of the convergence of the excavation as the overburden increases and as the support system remains unchanged. Negative trends with respect to overburden were found when double forepole grouted umbrella arch (FpdGUA) was investigated, as denoted by the 5 solid black outlined triangles in Fig. 18. These results, as well as the results found in Kim et al. (2005), indicate that the design of the umbrella arch support requires the inclusion of some type of factor associated with the remaining support system employed. Furthermore, the results illustrate that the circle geometry creates less surface settlement (when the umbrella arch is not installed) of 22% and 46% for the 6.5 m and 6.0 m diameter tunnels, respectively, when compared to the as-built case for the Istanbul metro. When an umbrella arch was installed for the 6.0 m and 6.5 m diameter tunnels, the reduction of surface settlement was found to be 53% and 58%, respectively. Therefore, the results of circular tunnels found that the forepole grouted umbrella arch (FpGUA) had less influence on reducing the surface settlement than those installed for a horseshoe tunnel. Similar results were found when the FpdGUA was simulated in the Istanbul model, and 73% and 71% reduction of surface settlement occurred for the 6.5 m and 6.0 m diameter tunnels, respectively.

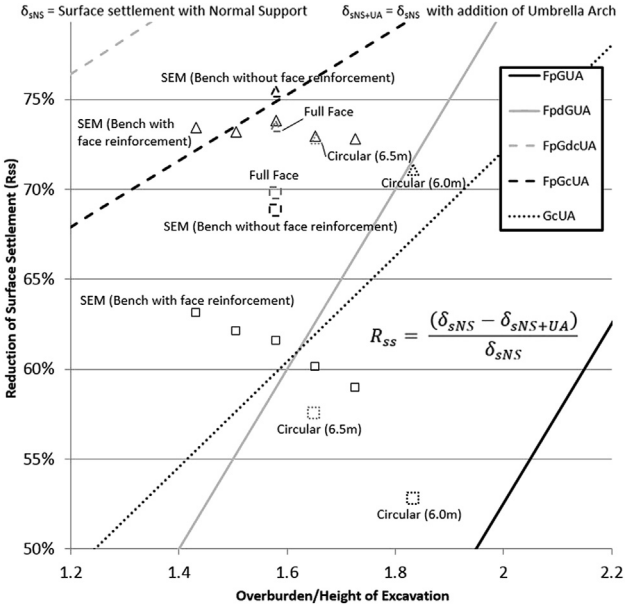

Fig. 18. Numerical analysis results from the Istanbul metro plotted on the subsidence management plot from the UASC. Squares denote analysis conducted with a FpGUA, and triangles denote a FpdGUA. SEM = sequential excavation method.

6. Optimisation methodology and validation

Both the literature and the numerical investigations provide findings which support the inclusion of numerical assessment for the spacing and overlap design parameters in the umbrella arch system, prior to analysis of the global response. Such numerical assessments are required as these design parameters are based on local failure mechanisms which remain difficult to be captured (and quantified) in a numerical analysis of the complete tunnel excavation. In the following sections, the authors will propose an optimisation methodology which employs numerical analysis to select design parameters. This optimisation will be conceptually validated using the worst squeezing case scenario captured at the Driskos tunnel at section 8 + 746. At this location, the FpGUA did not fail, so it is eligible as validation for the design methodology. The worst section (Chainage 8 + 746), however, included displacements far greater than the average parameters used in previous analysis. Therefore, further investigation is required and will be presented in the following section.

6.1. Driskos twin tunnel construction project

As previously stated, the preliminary properties conducted within this paper and used for the Driskos tunnel analyses, were found prior to the tunnel excavation. Upon excavation, it was discovered that at the selected location the squeezing of ground material was far greater than anticipated (Vlachopoulos, 2009). The maximum tunnel closure recorded during the top heading was found to be 210 mm (Egnatia Odos, 2001), along with primary-support failures along a stretch of the left bore (Chainage 8 + 500 to 8 + 800) (Grasso et al., 2005). From Chainage 8 + 657 to 8 + 746, monitoring data were collected and presented by Vlachopoulos (2009), as shown in Fig. 19. The calibration process was carried out from the worst case of convergence from in-situ data, Chainage 8 + 746. Despite of the data existing as an isolated condition, the forepole elements did not fail, rendering the design recommendation functional for these conditions. While the preliminary properties successfully captured the trend of most of the in-situ data at Chainages 8 + 657, 8 + 697, and 8 + 724, as illustrated in Fig. 19, they underestimated the displacement of the isolated condition at Chainage 8 + 746, despite of the numerical model not having included any support elements. A back analysis conducted by Marinos et al. (2006) on a similar rock mass found that the σ_{ci} value was greatly overestimated for this isolated case, and must be reduced from 26.25 MPa to 5–6 MPa for the given Driskos overburden. The reduction of rock mass parameters can be found in Table 4. This reduction allowed for displacements of an unsupported model analysis far greater than that of the in-situ supported model, as shown in Fig. 19. The authors have conducted a calibrated as-built numerical model simulation of the Driskos tunnel section 8 + 746, as shown in Fig. 20. Only the spacing and overlap design parameters, however, are altered within this investigation; complete optimisation for the other design parameters (ϕ_{fp} = 101 mm, t_{fp} = 6.3 mm, L_{fp} = 12 m, α_{fpa} = 160°, and α_{fp} = 5.73°) will not be conducted. It is important to note that the zero reading for the in-situ data was not taken till at least 10 m back from the tunnel face (as illustrated in Fig. 19), making it difficult to calibrate the numerical model to any displacement near the tunnel face.

6.2. Spacing assessment

As previously mentioned, an investigation is required to find the maximum spacing for the forepole elements within the umbrella

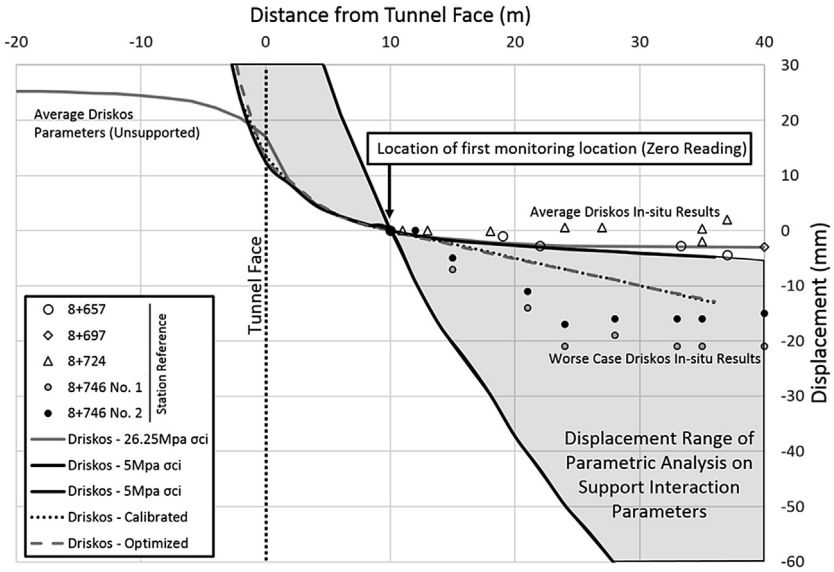

Fig. 19. Comparison of in-situ data to numerical results of unsupported model. Hollow markers denote typical recorded data and filled markers denote the isolated squeezing condition. The grey shaded region represents the range of possible solutions of supported model based on numerical parametric analysis of the isolated ground material found in Table 3

arch arrangement. Otani et al. (2008) proposed an experimental design spacing based on the diameter of the forepole and the friction angle of ground material. The result of this experimental design criterion theoretically maximised the height of the failure region to the radius of the forepole. However, this design did not take into consideration the effect of cohesion. The assessment from Doi et al. (2009) found that the friction angle had a minimal impact on the failure compared to the cohesion. In order to assess the possible maximum spacing, Doi et al. (2009) performed a trap door test using a discrete particle element model, PFC (Figs. 3a and 21a). They employed the forepole elements as rigid (fixed) particles and sequentially removed the boundary condition between and underneath the elements. As previously stated, Doi et al. (2009) captured the effect of cohesion and friction angle, which was then related to the local failure height between the forepole elements. This height, however, was not associated with any design standard to replace the work of Otani et al. (2008).

Based on the work of Stockl (2002), shown in Fig. 21b, Volkmann and Schubert (2007) indicated that the required spacing was designed to maintain local arching. In this event, the height of failure should not be an indication of the spacing design parameter, but instead be based on the forepole spacing ability to prevent ravelling type failure between forepole elements. This type of failure mechanism could not be captured in Doi et al. (2009) as the boundary conditions were not located in the centre of the forepole element. Doi et al. (2009) imposed a mirror on the outside edge of the model to simulate forepole elements with irregular spacing (i.e. side by side, space, side by side). This irregular spacing further resulted in a boundary arching effect, as shown in Fig. 21a.

Stockl (2002) performed a small scale physical experiment to illustrate two failure modes: local and global (Fig. 22). He illustrated that both of these failure modes could be captured within a comparable PFC numerical analysis (Fig. 21a). The authors decided to therefore illustrate this method through the creation of a similar type of analysis geared toward discovery of the optimum forepole spacing. Two such methods are illustrated within this paper, the first is a simplified model (continuum) while the second is an advanced model, such as the one proposed by Doi et al. (2009) and Stockl (2002).

6.2.1. Simplified model

The simplified model will be illustrated by employing the Phase2 modelling programme, based on a homogenous material, for the ground and element zones to represent the grout and forepole elements. The boundary conditions and mesh of the simplified model are illustrated in the top portion of Fig. 23, which also illustrates the resulting options for loading conditions (field stress and gravity). The bottom boundary stress condition is lowered from in-situ to zero. When the loading conditions were compared with the calibrated numerical results of Stockl (2002),

Table 4
Parameters used for numerical analysis of the as-built Driskos tunnel at Chainage 8 + 746 (Marinos et al., 2006; Vlachopoulos, 2009).

Shape	Height of excavation, H_e (m) (top/total)	In-situ stress (overburden) (m)	Excavated material
Horseshoe	8.78/11.70	106	Flysch ($GSI = 22$)

Hoek-Brown parameters			Mohr-Coulomb parameters		Modulus of elasticity (MPa)	Poisson's ratio
m	s	a	c (kPa)	φ (°)		
0.478	0.000172	0.538	118	21.3	681.1	0.25

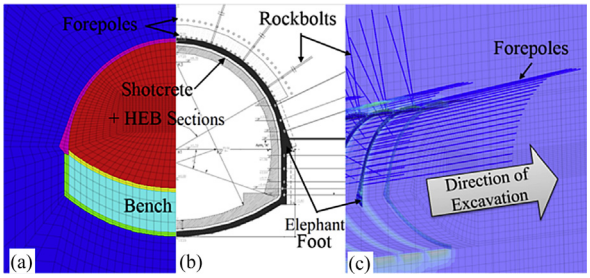

Fig. 20. Illustration of the numerical model and support layout of the Driskos tunnel. (a) Cross section image of the numerical model of the Driskos tunnel. (b) Support layout used at the Driskos tunnel project (Egnatia Odos, 1998). (c) Oblique image of the as-built design of Driskos tunnel with visual support element used for analysis. Only top heading is excavated.

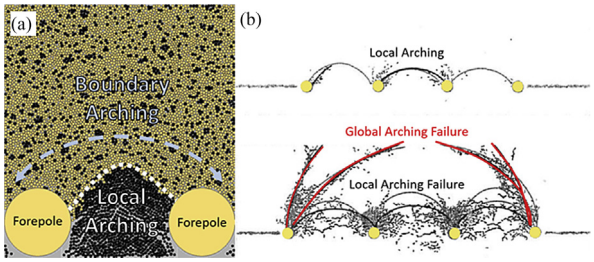

Fig. 21. PFC numerical modelling of forepole spacing. (a) Illustration of boundary arching effect of the ground caused by the imposed boundary conditions, modified after Doi et al. (2009). (b) Illustration of local arching and failures, modified after Stockl (2002).

the gravity driven stress condition represents reality more accurately due to the shear failure developed above the forepole elements. The overall results, however, tend to develop a comparable tension failure region once the bottom pressure boundary is completely removed. Furthermore, the Phase2 analysis is based on a continuum model, and the ground material cannot fall between the forepole elements, as illustrated in the model by Doi et al. (2009). Based on the rigidity of the forepole elements and the imposed boundary conditions, a local arching effect will be consistently achieved (within realistic spacing parameters). The model, however, is able to capture the tension failure region, which, in theory, would has fallen out during the excavation.

An analysis was conducted on the spacing based on the average Driskos tunnel parameters. The tension failure region was found to be greater than the radius of the forepole elements when the spacing was increased to 35 cm. This result agrees with the as-built design of an initial spacing of 30 cm for the forepole elements. The spacing of the forepole element, however, is not constant due to the angle of installation of the forepole elements. The forepoles at the Driskos tunnel project were installed at an angle of 5.73° which would result in a spacing of 36 cm after 8 m of excavation (the location of the next installation of forepole elements). An even greater spacing allowance could exist (44 cm) if the calculation included the 0.5% average deviation of drilling (Mager and Mocivnik, 2000). Therefore, as an alternative to Otani et al. (2008), the authors hypothesise that a more appropriate design standard would designate that the maximum design spacing of the forepole element be based on the failure region height, equalling the diameter of the forepole element, as was found to be the average in the Driskos tunnel case.

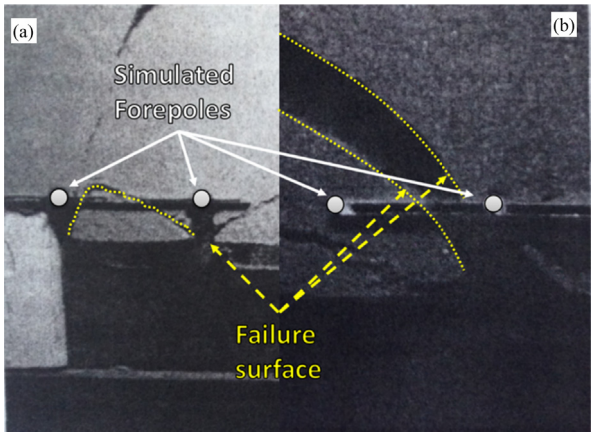

Fig. 22. Physical testing results of Stockl (2002). (a) Local failure between forepole elements. (b) Global arching failure across forepole elements.

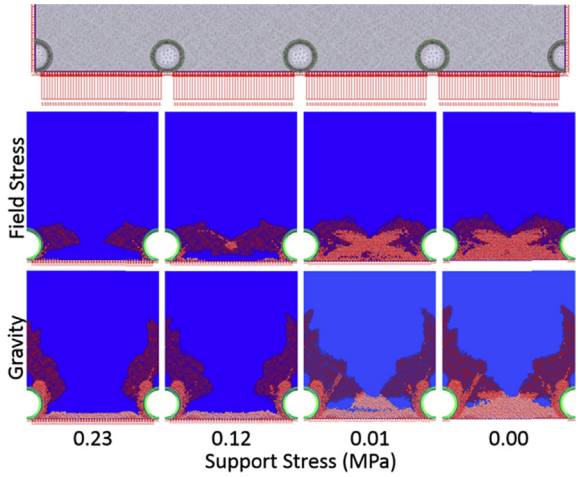

Fig. 23. Illustration of the simplified spacing assessment for a 114 mm diameter forepole elements with 50 cm spacing. Top – mesh and boundary conditions of numerical model; Middle – field stress driven failure region propagation; and Bottom – gravity driven failure region.

To further validate this failure region height, an analysis was carried out using the new properties for section 8 + 746 of the Driskos tunnel. It was concluded that the spacing could not be determined without consideration of the other support members and the effect of the tunnel face. The support pressure (bottom boundary condition) was reduced to the mobilised support pressure (0.32 MPa) based on convergence-confinement theory (Carranze-Torres, 2004; Hoek, 2007; Vlachopoulos and Diederichs, 2014). It was found through the simplification model that a local failure between the forepole elements would occur between a spacing of 40–45 cm, as shown in Fig. 25. This value is in agreement with the theoretical maximum spacing that occurred within section 8 + 746 (44 cm) due to a 0.5% installation deviation and installation angle of 5.73°.

6.2.2. Advanced models

The previous results may prove successful for homogenous materials, but may not be applicable for more complex material models where stability of the ground structure may be the governing factor (gravity driven failures). It is important to note that all of the further analysis of the spacing assessment will be performed with 50 cm of spacing in order to promote the various failure modes that potentially could be exhibited by advanced numerical models.

While advanced models are able to capture the structural failure mechanism, the models do require calibration of the material

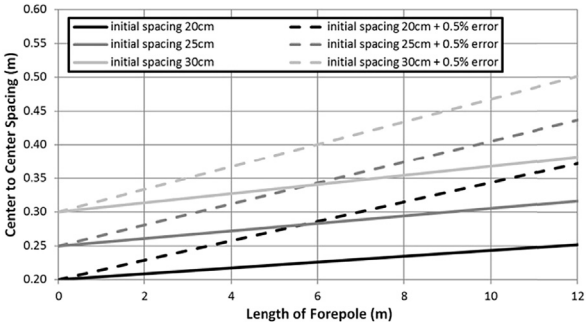

Fig. 24. Spacing assessment based on a 12 m length of forepole element, with a α_{fp} of 5.73°.

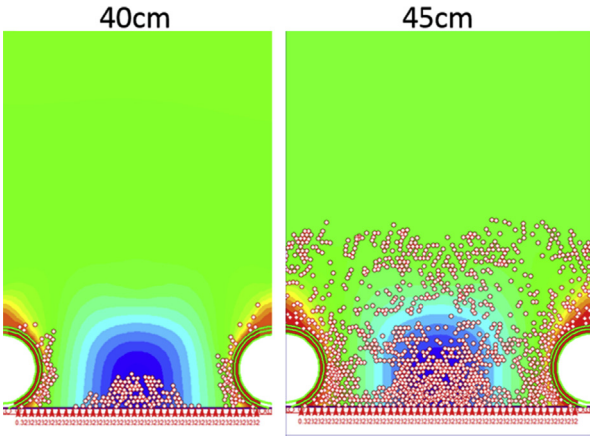

Fig. 25. Simplified analysis of the new Driskos tunnel spacing assessment, with an internal pressure of 0.32 MPa. Contour of displacement: Red = minimum (~0 mm); Blue = maximum; White dots denote tension failure. Shear failure is not shown.

parameters. Such calibration can be performed with the ground material simulated as a particle or discrete element model, or continuum (such as Phase2) model with simulated joints or Voronoi grains. Calibration is required to ensure proper interaction between particles or joints, as shown in Potyondy and Cundall (2004) for PFC models.

As an alternative to discrete particle codes, Fig. 26 provides an illustration of a Voronoi model and displays two of the four different automatic Voronoi mesh generations built into Phase2. The interaction parameters and the average size of the Voronoi model were held constant for the two different models, while the coefficient of uniformity was altered. It is apparent that the coefficient of uniformity has an additional impact on the design of the optimum forepole spacing, and should be taken into consideration for design. This Voronoi process can also be easily simulated with discrete element models.

When assessing the spacing of the forepole element, another aspect that must be taken into consideration during the design process is the joint network of the ground material. An illustration of the impact of the joints on the response of the spacing can also be found in Fig. 26. The top left side of Fig. 26 illustrates a hypothetical condition in which joints are offset by 90° but remain parallel and perpendicular to the tunnel boundary surface, respectively. The top right side of Fig. 26 illustrates a hypothetical condition where joints remain offset by 90° but are 45° from the tunnel boundary surface. It is apparent that if the numerical model was not constrained within a continuum approach, a triangular shape block would have failed between the two forepole elements until the "apparent arch" was formed. Similarly, on the left side, a possible rectangular block would have failed between the two forepole elements. With regard to the failure limit, however, it is not explicitly clear where the rectangular block failed or that to the exact height the apparent arch would have propagated to. This joint model process, which was simulated in Phase2 with an explicit joint boundary, could be easily simulated with UDEC, but is not illustrated within this paper.

Though relatively simple, these advanced models can provide great insight into the mechanical interaction which exists between the individual forepole elements and the ground. Due to the demands on time, this type of assessment is not economically feasible (time requirement) within a complete 3D numerical analysis of the tunnel excavation. All other parameters, however, are capable of assessment in terms of the global response of the umbrella arch system, such as the overlap of the forepole elements.

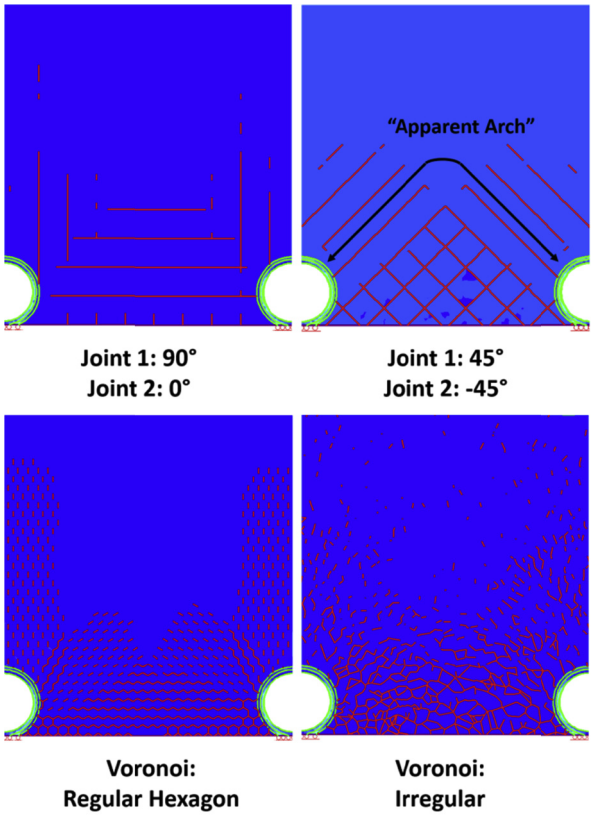

Fig. 26. Illustration of the use of Voronoi and joint sets models to define the failure region for a 50 cm forepole spacing with gravity driven stress condition. The red lines indicate the failure joint surface of the Voronoi mesh or joint surface.

6.3. Overlap assessment

As previously illustrated, the forepole element must be embedded past the disturbed zone ahead of the tunnel face. Within the numerical investigation of the Istanbul metro, the Rankine active failure block was a suitable approximation of the required overlap of the forepole elements of the umbrella arch. The approximation, however, does not include the impact of other face stabilising techniques. Limit equilibrium analysis could be taken into account for the other stabilising techniques. This type of analysis is outside the scope of this paper, but will be investigated in future research. Another approach available for assessment of the overlap requirement is the axisymmetric analysis as it requires merely hours for capturing, as opposed to days for a complete 3D numerical analysis. This axisymmetric analysis must be used with caution, however, as it is only truly applicable for installation of the forepole element in squeezing ground condition.

Axisymmetric analysis can be performed to illustrate the required overlap by assessing the distance from the tunnel face, along the tunnel boundary, to the outer limits of shear strain failure or the extent of plastic failure. An illustration of the extent of plastic failure can be found in Fig. 27. The additional face stabilising techniques can be simulated within the numerical analysis to capture their effect on the reduction of the required overlap. Structural supports within Phase2 analysis, however, cannot be simulated within axisymmetric analysis (except liners). Therefore, simplifications and/or approximations must be taken into consideration to simulate the face stabilising techniques. To illustrate simplifications and/or approximations, the authors have conducted an assessment on face reinforcement (soil nails) simulated as internal pressure

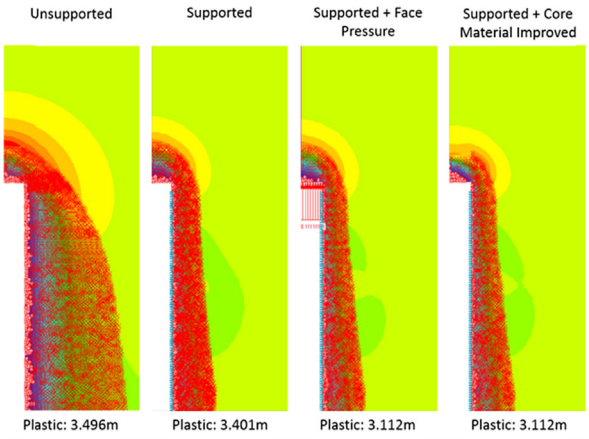

Fig. 27. Illustration of the impact of different supports (and simulations of support) on the shear failure distance from the tunnel face along the excavation profile boundary.

acting at the face and improved ground conditions (Fig. 27). As is illustrated from the numerical analysis results presented in Fig. 27, the support (shotcrete only) is capable of reducing the failure region ahead of the tunnel face. It is also apparent that face support (simulated by an applied pressure or improved ground condition) will further reduce the failure in the vicinity of the tunnel face. Therefore, before embarking on a time consuming 3D numerical analysis, a simple axisymmetric model can be substituted to find the failure region ahead of the tunnel face and to help define the overlap required for successive umbrella arches.

The requirement for overlap for a squeezing ground condition is completely different from that for a subsidence driven condition. To ensure optimal use of the support in terms of reducing surface settlement, it is required that the next umbrella arch of support is installed while the embedded end of the current umbrella is in stable ground. In squeezing ground conditions, the plasticity zone is fair greater, and it remains impractical to install an overlap with this guideline. Furthermore, the rationale for installing forepoles under squeezing ground conditions is to transfer the stresses longitudinally away from the tunnel face which will, in turn, reduce degradation of the rock mass through confinement. Therefore, minimal embedment length, as opposed to subsidence, is required. From these considerations, the authors proposed that the selection of the overlap should be based on the maximum distances of the tension failure in front of the tunnel face. The required overlap, based on section 8 + 746, was found to be 1.488 m for the unsupported model and 2.412 m for the supported model, as shown in Fig. 28. The design for the overlap is also based on the pre-

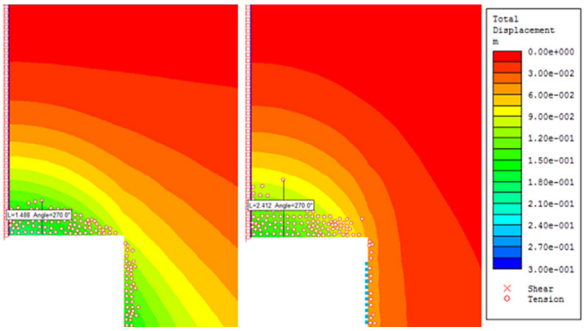

Fig. 28. Tension failure of an axisymmetric analysis for the Driskos section 8 + 746. Left: unsupported. Right: supported (shotcrete only). Shear failure is shown within image.

determined excavation step, which was 2 m. Therefore, the optimum overlap should be 2 m.

6.4. Driskos tunnel design optimisation

As previously stated in Section 6.1, without changing/optimising the remaining design parameters, the result of the optimised initial spacing was found to be 25 cm, based on a maximum spacing of 40 cm with an overlap of 2 m for a 12 m long forepole element, as illustrated in Fig. 24. As it was shown in Fig. 19, a "calibrated" numerical model was found within the range of the parametric analysis of support interaction parameters. This calibrated model was created attempting to match the displacement trend from the worst case in-situ parameters. The exact profile was not able to be captured, which was attributed to simulating a homogenous material throughout the whole numerical model, as well as not simulating the niche or saw-tooth profile. However, the results are within reasonable limits for comparison of the optimised simulations. During the optimisation of the umbrella arch support, layout of the forepole elements with the simulated overall displacement profile did not change significantly, as shown in Fig. 19. The maximum resulting moment comparison, conversely, found that there was a 27.0% and −26.9% difference of positive and negative moment, respectively. This large difference of moment, however, was insignificant because the maximum resulting moment was over 100 orders of magnitude greater than forepole capacity found by Volkmann and Dolsak (2014). This finding is an indication either that the forepole elements stiffness was over designed or required to provide safe and effective excavation process for squeezing ground conditions. Furthermore, the optimised design resulted in an 8% reduction in tangential stress acting on the tunnel walls.

Furthermore, an evaluation of the economic impact of this design change was conducted. For each umbrella arch installed, 10 more forepoles would be employed to keep the same α_{fpa} when changing the initial spacing from 30 cm to 25 cm. This increase in forepole elements would require more time to install, slowing the excavation process. However, the decrease in the requirement for L_{fpo} over a 40 m stretch (before the next umbrella arch is installed) results in one fewer umbrella arch installation set-up when changing L_{fpo} from 4 m to 2 m. This optimised design results in one fewer umbrella arch installation set-up and 10 fewer forepole elements total employed over 40 m of excavation. Therefore this optimisation of design will decrease the time required to install by 10 fewer forepoles and one less set-up of the forepole jumbo for each 40 m of excavation, increasing the excavation rate.

7. Summary and conclusions

This paper has investigated relevant concepts with respect to the employment of numerical techniques and analysis in support of the design of umbrella arch systems. An examination of 2D numerical analysis determined that such techniques were mechanistically incorrect in capturing the global response of such support systems, yet efficient in capturing localised failure between support elements and with respect to support-ground interaction; meanwhile, 3D analysis proved necessary for the capture of the global response of forepoles within an umbrella arch system. Through a detailed illustration of multiple, relevant sensitivity and parametric studies highlighted in the multiple sections of this paper, the importance of interaction parameters was emphasised, and procedures of recommended calibration processes were presented for both shallow and deep tunnelling excavation scenarios. The most sensitive parameters were determined to be k_n, k_s, and C_n. The individual influence of each respective design parameter on the global response was also presented.

The length of overlap, L_{fpo}, was found to be related to the investigated failure region ahead of the tunnel face. For subsidence driven (shallow) designs, L_{fpo} must be at a distance past the plastic failure region. For squeezing ground, L_{fpo} must be at a distance past unstable ground sections, with the extent of tension failure assumed. The axisymmetric analysis was found to provide a quick approximation of this design parameter.

The coverage angle of the forepole elements, α_{fpa}, was found to exert a greater influence on the global response of a system when compared with the centre to centre spacing of the forepole elements, S_{cfp}. The S_{cfp} was found to be a critical design parameter, yet one that could not be easily captured in full scale 3D numerical analysis. The authors have therefore proposed a 2D analysis approach in order to capture the maximum spacing, based on typical size/stiffness of the forepole elements (diameter, ϕ_{fp}, and thickness, t_{fp}), and the angle of installation α_{fp}. Such approaches can be employed for both squeezing ground conditions (continuum model) and gravity driven failure (particle, discrete, and jointed continuum models).

The increase of the angle of installation from the horizontal was found to slightly decrease the convergence of the continuous profile of the tunnel excavation. This result, however, proved to be relatively insignificant for a "saw-tooth" profile excavation due to the increased requirements of other support members. As noted previously, the umbrella arch with forepole elements is always employed in conjunction with other temporary support systems; these additional systems also have an influence on the global response of the complete system that must also be determined.

In conclusion, this paper presented the use of numerical techniques in order to add value to the understanding of the influences of design parameters on forepole elements used within an umbrella arch system. The paper also provided an overview of suggested, sound numerical modelling procedures for support systems, optimisation of design, and the comprehensive performance of full 3D analysis of preliminary design.

It should be noted, however, that sound engineering judgement and a comprehensive understanding of the fundamentals associated with geotechnical, mechanical and numerical analysis factors are always prerequisites prior to conducting a preliminary design for tunnel construction of this nature. A designer must understand the limitations associated with the numerical tools combined with the accuracies related to obtaining sound geotechnical data (i.e. input and interaction parameters, site-specific factors, etc.).

Conflict of interest

The authors wish to confirm that there are no known conflicts of interest associated with this publication and there has been no significant financial support for this work that could have influenced its outcome.

Acknowledgement

This work has been funded by the Natural Sciences and Engineering Research Council of Canada, the Department of National Defence (Canada) as well as graduate funding obtained at Queen's University and the Royal Military College of Canada. A special thanks goes to Ehsan Ghazvinian for his help with the Voronoi and PFC considerations.

References

Broch E, Lu M, Trinh QN. Three dimensional modelling of a tunnel cave-in and spiling bolt support. In: Leung CF, Zhou YX, editors. Proceedings of the ISRM international symposium 2006 and the 4th Asian rock mechanics symposium. Singapore: World Scientific Publishing Co., Pte. Ltd; 2006.

Carranze-Torres C. Elasto-plastic solution of tunnel problems using the generalized form of the Hoek-Brown failure criterion. International Journal of Rock Mechanics and Mining Sciences 2004;41(3):480–91.

Carrieri G, Grasso P, Mahtab A, Pelizza S. Ten years of experience in the use of umbrella-arch for tunneling. In: Proceedings of the international congress on soil and rock improvement in underground works; 1991. p. 99–111.

Doi Y, Otani T, Shinji M. The optimum distance of roof umbrella method for soft ground by using PFC. In: Ma GW, Zhou YX, editors. Analysis of Discontinuous Deformation: New Developments and Applications. Singapore: Research Publishing Services; 2009. p. 461–8.

Egnatia Odos SA. Geological study by asproudas and cooperates consultants. 1998 (in Greek).

Egnatia Odos SA. The appropriate use of geological information in the design and construction of the Egnatia motorway tunnels, tunnel construction in Greece. Technical notes of the National Technical University of Athens. 2001.

Federal Highway Administration (FHA). Technical manual for design and construction of road tunnels–civil elements. 2009. http://www.fhwa.dot.gov/Bridge/tunnel/pubs/nhi09010/errata.cfm.

Funatsu T, Hoshino T, Sawae H, Shimizu N. Numerical analysis to better understand the mechanism of the effects of ground supports and reinforcements on the stability of tunnels using the distinct element method. Tunnelling and Underground Space Technology 2008;23(5):561–73.

Grasso P, Scotti G, Blasini G, Pescara M, Floria V, Kazilis N. Successful application of the observational design method to difficult tunnel conditions–Driskos tunnel. In: Erdem Y, Solak T, editors. Underground Space Use: Analysis of the Past and Lessons for the Future. 2005. p. 463–70.

Hoek E. Big tunnels in bad rock: 2000 Terzaghi lecture. ASCE Journal of Gotechnical and Geoenvironmental Engineering 2001;127(9):726–40.

Hoek E. Rock-support interaction analysis for tunnels in weak rock masses. In: Evert H, editor. Practical Rock Engineering. Rocscience; 2007.

Hoek E. Support for very weak rock associated with faults and shear zones. In: International symposium of rock and support and reinforcement practice in mining. Kalgoorlie, Australia; 1999.

Hun Y. Stability and collapse mechanism of unreinforced and forepole reinforced tunnel headings. PhD Thesis. Singapore: National University of Singapore; 2011.

Itasca Consulting Group Inc. Fast Lagrangian analysis of continua in 3 dimensions, version 4.0. Minneapolis: Itasca Consulting Group Inc.; 2009.

Itasca Consulting Group Inc. Particle flow code, PFC v3.0. Minneapolis: Itasca Consulting Group Inc.; 2002.

Kim SH, Baek SH, Moon HK. A study on the reinforcement effect of umbrella arch method and prediction of tunnel crown and surface settlement. In: Erdem Y, Solak T, editors. Underground Space Use: Analysis of the Past and Lessons for the Future. London: Taylor & Francis; 2005. p. 245–51.

Mager W, Mocivnik J. Modern casing technology sets a milestone in drilling and ground anchoring. Felsbau 2000;18:43.

Marinos V, Fortsakis P, Prountzopoulos G. Estimation of rock mass properties of heavily sheared flysch using. In: IAEG2006. The Geological Society of London; 2006. Paper No.314.

Ocak I. Control of surface settlement with umbrella arch method in second stage excavation of Istanbul metro. Tunnelling and Underground Space Technology 2008;23(6):674–81.

Oke J, Vlachopoulos N, Diederichs MS. Improved input parameters and numerical analysis techniques for temporary support of underground excavations in weak rock. In: RockEng. Edmonton; 2012.

Oke J, Vlachopoulos N, Diederichs MS. Modification of the supported longitudinal displacement profile for tunnel face convergence in weak rock. In: 47th US rock mechanics/geomechanics symposium. San Francisco: American Rock Mechanics Association; 2013b.

Oke J, Vlachopoulos N, Diederichs MS. Semi-analytical model of an umbrella arch employed in hydrostatic tunnelling conditions. In: 48th US rock mechanics/geomechanics symposium. Minneapolis: American Rock Mechanics Association; 2014b.

Oke J, Vlachopoulos N, Diederichs MS. The reduction of surface settlement by employing umbrella arch systems. In: GeoMontreal 2013. Montreal: Canadian Geotechnical Society; 2013a.

Oke J, Vlachopoulos N, Diederichs MS. The reduction of surface settlement by employing umbrella arch systems for different excavation methods. In: The ISRM European rock mechanics symposium–EUROCK2014. Vigo: International Society of Rock Mechanics; 2014c.

Oke J, Vlachopoulos N, Marinos V. The pre-support nomenclature and support selection methodology for temporary support systems within weak rock masses. Journal of Geotechnical and Geological Engineering 2014a;32(1):97–130.

Otani T, Shin JI, Chijiwa T. Proposal of numerical model and the determination method of design parameters for pipe roofing method. Daboku Gakkai Ronbunshuu 2008;64(4):450–62.

Peila D. Forepoling design. In: Ground Improvement, Pre-support and Reinforcement Short Course. Geneva: International Tunnelling and Underground Space Association (WTC 2013); 2013.

Potyondy DO, Cundall PA. A bonded-particle model for rock. International Journal of Rock Mechanics and Mining Sciences 2004;41(8):1329–64.

Rocscience Inc.. Phase2 v7. Toronto, Canada: Rocscience Inc; 2010.

Rocscience Inc.. Phase2 v8. Toronto, Canada: Rocscience Inc.; 2013.

Shin JH, Choi YK, Kwon OY, Lee SD. Model testing for pipe-reinforced tunnel heading in a granular soil. Tunnelling and Underground Space Technology 2008;23(3):241–50.
Song KI, Cho GC, Chang SB, Lee IM. Beam-spring structural analysis for the design of a tunnel pre-reinforcement support system. International Journal of Rock Mechanics and Mining Sciences 2013;59:139–50.
St. John CM, Van Dillen DE. Rockbolts: a new numerical representation and its application in tunnel design. In: 24th US symposium on rock mechanics. New York: Association of Engineering Geologists; 1983. p. 13–26.
Stockl C. Numerische Berechnung der Tragwirkung von Rohrschirmen mit PFC-2D. MS Thesis. Graz: Graz University of Technology; 2002 (in Germany).
Trinh QN. Analyses of a cave-in problem in a hydropower tunnel in Vietnam. PhD Thesis. Trondheim, Norway: Norwegian University of Science and Technology; 2006.
Vlachopoulos N, Diederichs MS, Marinos V, Marinos P. Tunnel behaviour associated with the weak Alpine rock masses of the Driskos twin tunnel system, Egnatia Odos Highway. Canadian Geotechnical Journal 2013;50(1):91–120.
Vlachopoulos N, Diederichs MS. Appropriate uses and practical limitations of 2D numerical analysis of tunnels and tunnel support response. Geotechnical and Geological Engineering 2014;32(2):469–88.
Vlachopoulos N. Back analysis of a tunnelling case study in weak rock of the alpine system in northern Greece: validation and optimization of design analysis based on ground characterization and numerical simulation. PhD Thesis. Kingston, Ontario: Queens University; 2009.
Volkmann G. Rock mass-pipe roof support interaction measured by chain inclinometers at the Birgltunnel. In: Proceedings of international symposium on geotechnical measurements and modeling. Karlsruhe: A.A. Balkema; 2003. p. 105–9.
Volkmann GM, Dolsak W. Development of innovative connections for pipe umbrella support systems. In: Tunnels for a Better Life, Proceedings of the World Tunnel Congress. Iguassu Falls, Brazil; 2014.
Volkmann GM, Schubert W, Button EA. A contribution to the design of tunnels supported by a pipe roof. In: 50 Years of rock mechanics—Landmarks and future challenges, Proceedings of the 41st US symposium on rock mechanics. Golden, Colorado; 2006.
Volkmann GM, Schubert W. A load and load transfer model for pipe umbrella support. In: Zhao J, Labiouse V, Dudt JP, Mathier JF, editors. Rock mechanics in civil and environmental engineering, proceedings of the European rock mechanics symposium (EUROCK) 2010. Rotterdam, Niederlande: CRC Press/A.A. Balkema; 2010. p. 379–82.
Volkmann GM, Schubert W. Contribution to the design of tunnels with pipe roof support. In: Rock mechanics in underground construction: ISRM international symposium 2006: 4th Asian rock mechanics symposium. Singapore: World Scientific Pub. Co. Inc.; 2006a.
Volkmann GM, Schubert W. Geotechnical model for pipe roof supports in tunneling. In: Proceeding of the 33rd ITA-AITES World tunneling congress, underground space—the 4th dimension of metropolises. London: Taylor & Francis Group; 2007. p. 755–60.
Volkmann GM, Schubert W. Optimization of excavation and support in pipe roof supported tunnel sections. Tunnelling and Underground Space Technology 2006b;21(3–4):404.
Wang H, Jia J. Analytical method for mechanical behaviors of pipe roof reinforcement. In: 2008 International conference on information management, innovation management and industrial engineering. Institute of Electrical and Electronics Engineers (IEEE); 2008. p. 352–7.
Yasitli NE. Numerical modeling of surface settlements at the transition zone excavated by New Austrian tunneling method and umbrella arch method in weak rock. Arabian Journal of Geosciences 2013;6(7):2699–708.

Mr. Jeffrey Oke obtained a Bachelor's degree in Civil Engineering from the Royal Military College of Canada, Kingston, Ontario (2010). He is expected to finish his PhD at Queen's University in 2015, specializing in Umbrella Arch support systems, under the supervision of Dr. Nicholas Vlachopoulos and Dr. Mark Diederichs. Jeffrey's research objectives are to create/develop: standardization of nomenclature of the umbrella arch systems; design selection chart for umbrella arch systems; semi-analytical model for umbrella arch systems employed in squeezing ground conditions; and optimization of umbrella arch systems employed in squeezing ground conditions.